



FLAME: Flow Enhanced Legendre Memory Models for General Time Series Forecasting

Xingjian Wu¹ Hanyin Cheng¹ Xiangfei Qiu¹ Zhengyu Li¹ Jilin Hu¹ Chenjuan Guo¹ Bin Yang¹

Abstract

In this work, we introduce **FLAME**, a family of extremely lightweight and capable Time Series Foundation Models, which support both deterministic and probabilistic forecasting via generative probabilistic modeling, thus ensuring both efficiency and robustness. FLAME utilizes the Legendre Memory for strong generalization capabilities. Through adapting variants of Legendre Memory, i.e., translated Legendre (LegT) and scaled Legendre (LegS), in the Encoding and Decoding phases, FLAME can effectively capture the inherent inductive bias within data and make efficient long-range inferences. To enhance the accuracy of probabilistic forecasting while keeping efficient, FLAME adopts a Normalization Flow based forecasting head, which can model the arbitrarily intricate distributions over the forecasting horizon in a generative manner. Comprehensive experiments on well-recognized benchmarks, including TFSM-Bench and ProbTS, demonstrate the consistent state-of-the-art zero-shot performance of FLAME on both deterministic and probabilistic forecasting tasks.

1. Introduction

Time Series Forecasting is a critical and widely studied task due to the attractive charm of peeking future, which helps make significant values in various fields through planning ahead. While, time series dances like a *flame* – it is hard to accurately capture the deterministic rules. Therefore, to control risks and make reasonable decisions, quantifying uncertainties through Probabilistic Time Series Forecasting (PTSF) is a more reliable approach, which is continuously explored for decades from statistical approaches (Godaheva et al., 2021a; Box & Pierce, 1970) with solid theories and

Preprint. ¹School of Data Science and Engineering, East China Normal University, Shanghai, China. Correspondence to: Bin Yang <byang@dase.ecnu.edu.cn>.

A preprint version under peer-review.

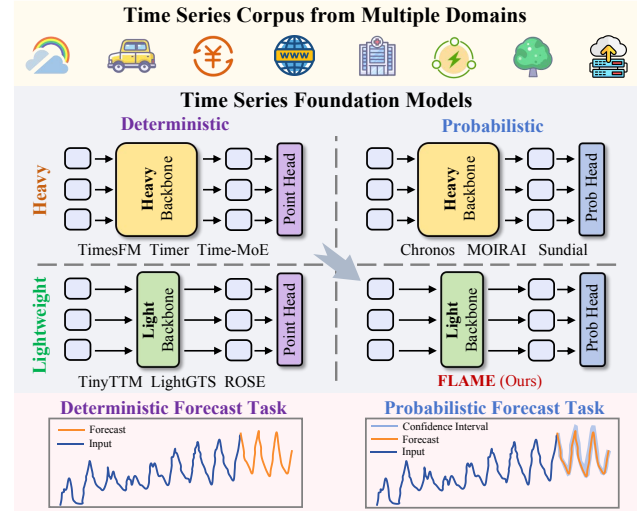


Figure 1. FLAME is pretrained on Time Series Corpus from Multiple Domains, possessing a *lightweight* backbone while supporting generative *probabilistic* forecasting.

interpretability to data-driven approaches (Nie et al., 2023; Qiu et al., 2025e; Wu et al., 2025b) with strong fitting capability. Among them, deep learning models (Nie et al., 2023; Qiu et al., 2025e; Wu et al., 2025b) show outstanding impressive performance on in-distribution tasks through effectively capturing the inherent dynamics within raw data. Inspired by the success of pretrained models in other domains such as CV (Khan et al., 2022; Liu et al., 2021) and NLP (Liu et al., 2024a; Achiam et al., 2023) with strong generalization capabilities, a surge of pretrained time series foundation models (Liu et al., 2024c; Das et al., 2024; Gao et al., 2024; Shi et al., 2024; Wang et al., 2025b;c) are developed for out-of-distribution tasks, demonstrating promising trends.

Recent studies on time series foundation models (Woo et al., 2024; Shi et al., 2024; Wang et al., 2025b; Liu et al., 2025d) have achieved some progress in exploiting the generalization capabilities and exhibit excellent forecasting performance in zero-shot scenarios. Their generalization capabilities mainly come from two perspectives—see Figure 1: 1) some works make efforts in devising appropriate Transformer-based ar-

chitectures, and expanding the parameters to Hundreds-Million- or Billion-Scale (Shi et al., 2024; Ansari et al.; Woo et al., 2024; Das et al., 2024), or with the help of the massive parameters from LLMs (Zhou et al., 2023; Jin et al., 2024) and ViTs (Chen et al., 2024a). Though these works achieve excellent performance in zero-shot scenarios, they consume a lot in inference under limited resources, and some of them are even slower than training end-to-end supervised models from scratch, thus *hindering the efficiency and practicality*; 2) another branch of works explore the effective capture of inductive bias within data, with meticulously-designed lightweight structures (Ekambaram et al., 2024; Gao et al., 2024; Wang et al., 2025b) but strong generalization capabilities. However, although they demonstrate strong performance in deterministic forecasting tasks, they *lack the support of probabilistic forecasting*. Moreover, predicting accurate distributions over the forecasting horizon is difficult because assuming prior distributions like Isotropic Gaussian Distributions constrains the modeling capabilities of real data distributions. On the other hand, modeling arbitrary complex distributions relies on generative mechanisms (Li et al., 2017; Kollovich et al., 2023), which may increase the model complexity and hinder the efficiency.

As shown in Figure 1, our proposed **FLAME** pioneers the exploration of *lightweight* time series foundation models capable of *both deterministic and probabilistic forecasting*. To enhance the generalization capability while keeping lightweight, we utilize the *Legendre Memory* (Voelker et al., 2019; Gu et al., 2020) in both Encoding and Decoding phases to capture the inherent inductive bias within data, which contributes to a lightweight but strong framework. Originating from ordinary differential equations (ODEs) and characterized by orthogonal legendre polynomials, the Legendre Memory has been utilized in control theory to model continuous time-delay systems (Richard, 2003) for several decades, which has the potential to compress time series of varying lengths into vectors of the same size. This helps ensuring lightweight, and we employ Legendre Memory in both the encoder and decoder.

First, in the pretraining process of time series foundation models, the inherent periods and trends of data from distinct domains can lead to complex local characteristics but the patching technique cannot handle this due to the fixed receptive field. This inspires us to devise a *Local-Perception* module to unlock the power of Legendre Memory in integrating intricate and varying local characteristics within data as the supplement environmental semantic information to patched tokens. Second, we also adopt the Structured State-Space Duality (SSD (Dao & Gu, 2024)) layers in the decoding phase, which utilizes the Legendre Memory to initialize the state transition matrices (Gu et al., 2020), excelling at modeling long time series based on its selective

states and adaptive memory utilization.

Besides the adaptations of Legendre Memory, we also devise a *Flow-based Head* to support generative probabilistic forecasting. Specifically, we focus on token-wise modeling, which constructs the distributions over dozens of time series points at once, and using the Flow-based Head driven by normalization flow (Rasul et al., 2021b; Durkan et al., 2019) can preserve both considerable efficiency and interpretability compared with prevailing diffusion models (Kollovich et al., 2023; Rasul et al., 2021a). Additionally, we also devise to capture the token-wise causality in the Flow-based Head, which is important but neglected in current decoding methods (Liu et al., 2025d; 2024c; Shi et al., 2024), and this can help preserve temporal dependencies within tokens to boost the fine-grained modeling. Through these adaptations, the Flow-based Head can preserve both the accuracy and efficiency through constructing lightweight couple layers to simulate the reversible conditional transfer process from fixed prior Gaussian distributions to any complex real-data distribution. With the Legendre Memory and Flow-based Head facilitating the strong generative paradigm, FLAME can make extreme fast and accurate probabilistic forecasts. Our contributions are summarized as:

- We present **FLAME**, a family of **Flow** enhanced Legendre **Memory** Foundation Models, including three parameter versions, i.e., 2M, 6M, 10M. Even the largest version of FLAME (10M) is far more lightweight than other time series foundation models which supports both deterministic and probabilistic forecasting.
- We adapt the Legendre Memory to enhance the generalization capability. Both the Local-Perception Module and SSD-Decoder are driven by Legendre Memory and able to adaptively utilize the inductive bias within data.
- We devise the Flow-based Head to model the intricate token-wise distributions over the forecasting horizon, considering the causality within tokens, with strong efficiency and accuracy.
- Experimentally, FLAME achieves state-of-the-art zero-shot performance on both deterministic and probabilistic forecasting benchmarks, including TSFM-Bench (Li et al., 2025c) and ProbTS (Zhang et al., 2024), demonstrating a strong out-of-the-box tool of decision intelligence. The resources are available at <https://anonymous.4open.science/r/FLAME-D83F>.

2. Legendre Memory

When modeling sequence data with recurrent networks, “memory” is a common concept denoting the online compression capability of historical observations. Among them, Legendre Memory (Voelker et al., 2019; Gu et al., 2020) is

a kind of continuous online function approximation, which utilizes orthogonal Legendre polynomials to compress the continuous-time history f into state vectors m with fixed sizes. From the perspective of *Real Analysis*, given a time-varying measure $\mu^{(t)}$ and a high-order polynomial operator, recent history f can be compressed into state vectors m under certain approximation error (Gu et al., 2020). When the operator is the Legendre polynomial, there exists two common time-varying measures: *translated Legendre (LegT)* and *scaled Legendre measure (LegS)*.

LegT assigns uniform weights to the most recent history $[t - \theta, t]$, where θ denotes the length of the sliding windows, or the length of history that is being summarized:

$$\text{LegT} : \mu^{(t)}(x) = \frac{1}{\theta} \mathbb{I}_{[t-\theta, t]}(x) \quad (1)$$

Under the LegT measure, the process of compressing the historical information f into state vectors m can be represented as solving d coupled linear time-invariant ODEs:

$$m'(t) = -Am(t) + Bf(t), \quad (2)$$

$$B_n = \frac{1}{\theta}(2n+1)(-1)^n, \quad (3)$$

$$A_{nk} = \frac{1}{\theta} \begin{cases} (-1)^{n-k}(2n+1) & \text{if } n > k \\ -2n+1 & \text{if } n \leq k \end{cases}, \quad (4)$$

where $A \in \mathbb{R}^{d \times d}$, $B \in \mathbb{R}^{d \times 1}$ are optimal parameters derived through the use of Padé approximant (Padé, 1892; Voelker, 2019). In the forward process, the sequence of $[t - \theta, t]$ can be compressed into the memory cell $m(t) \in \mathbb{R}^d$ in a recurrent mode using discretized Formula (2):

$$m_t = \bar{A}m_{t-1} + \bar{B}f_t, \quad (5)$$

$$\bar{A} = I - (\Delta t/\theta)A, \bar{B} = (\Delta t/\theta)B, \quad (6)$$

where \bar{A} and \bar{B} can be obtained through zero-order hold (ZOH). And the ‘‘memory’’ lies in the capability of using $m(t)$ to recover all the past history f of $[t - \theta, t]$, thus can describe a θ time-delay system (Richard, 2003):

$$f(t - \theta') \approx \sum_{i=0}^{d-1} \mathcal{P}_i \left(\frac{\theta'}{\theta} \right) m_i(t), \quad 0 \leq \theta' \leq \theta, \quad (7)$$

$$\mathcal{P}_i(r) = (-1)^i \sum_{j=0}^i \binom{i}{j} \binom{i+j}{j} (-r)^j, \quad (8)$$

where $\mathcal{P}_i(r)$ is the i -th shifted Legendre polynomial (Voelker et al., 2019). According to Theorem 2.1 (Gu et al., 2020), larger number d of Legendre Polynomials basis leads to more accurate approximation.

Theorem 2.1. *If $F(x)$ is L -Lipschitz, then $\|F_{[t-\theta, t]}(x) - f_{[t-\theta, t]}(x)\|_{\mu^{(t)}} \leq \mathcal{O}(\theta L/\sqrt{d})$. Moreover, if $F(x)$ has k -th order bounded derivatives, we have $\|F_{[t-\theta, t]}(x) - f_{[t-\theta, t]}(x)\|_{\mu^{(t)}} \leq \mathcal{O}(\theta^k d^{-k+1/2})$.*

Compared with LegT, LegS assigns uniform weights to all history $[0, t]$ to support the compression of the entire history:

$$\text{LegS} : \mu^{(t)}(x) = \frac{1}{t} \mathbb{I}_{[0, t]}(x) \quad (9)$$

Under the LegS measure, the compressing process is:

$$m'(t) = -\frac{1}{t} Am(t) + \frac{1}{t} Bf(t), \quad (10)$$

$$B_n = (2n+1)^{\frac{1}{2}}, \quad (11)$$

$$A_{nk} = \begin{cases} (2n+1)^{1/2}(2k+1)^{1/2} & \text{if } n > k \\ n+1 & \text{if } n = k \\ 0 & \text{if } n < k \end{cases}, \quad (12)$$

where $A \in \mathbb{R}^{d \times d}$ and $B \in \mathbb{R}^{d \times 1}$ can also be discretized as Formula (5) and Formula (6).

3. FLAME

FLAME adopts the Channel-Independent (Nie et al., 2023) pretraining paradigm, and each variable is preprocessed through Instance Normalization (Ulyanov et al., 2016) to mitigate the value discrepancy. As shown in Figure 2, FLAME utilizes the Re-Norm (Kim et al., 2021) to further mitigate the statistical differences between inputs and forecasts, and its backbone mainly consists of three modules: 1) Encoding, including Time Series Tokenization, Local-Perception, and MSA-Encoder, which tokenize the time series and enhance them through fusing the local environmental information with LegT; 2) Decoding, including LegS based SSD-Decoder and MCA-Enhancer, which utilize the SSD layers and MCA layers to make long-term inference; 3) Flow-based Head, which leverages the Normalization Flow to support generative probabilistic forecasting.

3.1. Encoding

3.1.1. TIME SERIES TOKENIZATION

In the pretraining Time Series Corpus, all data are preprocessed into univariate time series and received by FLAME in a Channel-Independent paradigm. Following the commonly used patching technique, which is first introduced by Triformer (Cirstea et al., 2022), we first divide each univariate time series $X \in \mathbb{R}^T$ into non-overlapping time series patches:

$$X^P = [h_1, h_2, \dots, h_n], \quad (13)$$

where $X^P \in \mathbb{R}^{n \times p}$ are the patches, $n = \lceil T/p \rceil$ denotes the patch number and p is the patch size. $h_i \in \mathbb{R}^p$ is the i -th patch. Subsequently, we use a linear layer: $\mathbb{R}^p \rightarrow \mathbb{R}^d$ to transform the patches to tokens:

$$X^{\text{token}} = [\text{linear}(h_1), \text{linear}(h_2), \dots, \text{linear}(h_n)], \quad (14)$$

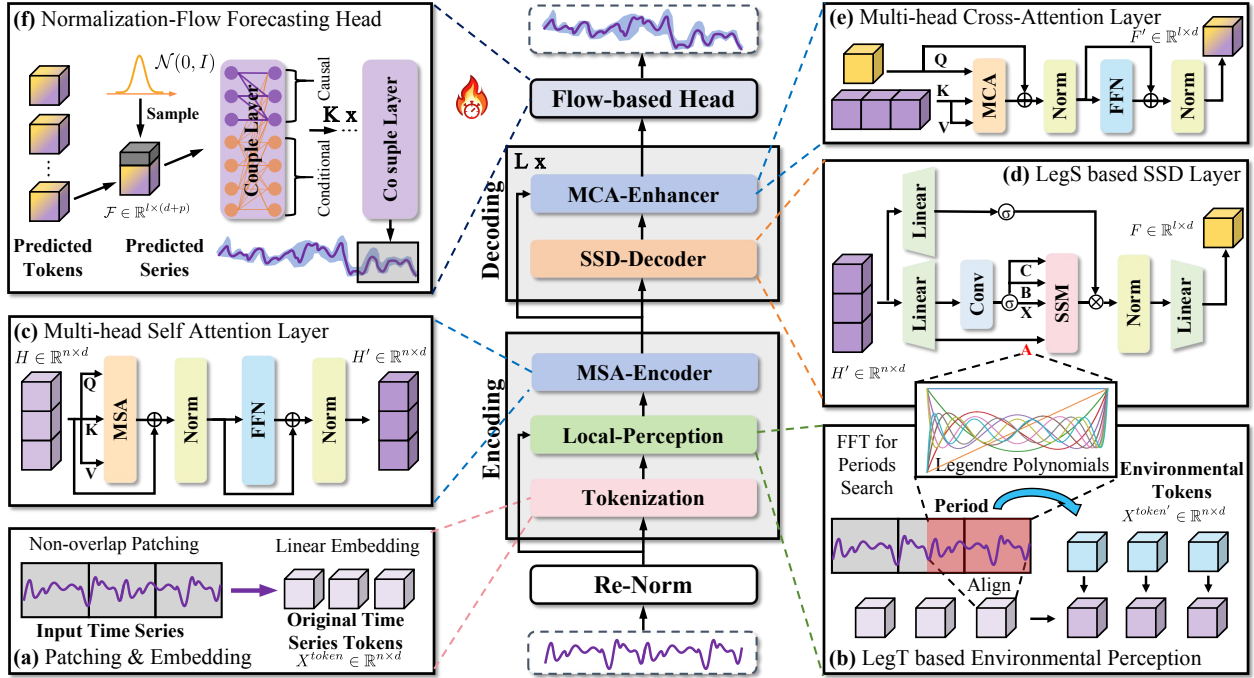


Figure 2. The overall framework of FLAME. The data flow follows the sequence of (a) - (f).

where $X^{token} \in \mathbb{R}^{n \times d}$ are the embedded time series tokens. Patch-wise tokens preserve semantic information and reduce the number compared with point-based tokens, thus enhancing efficiency.

3.1.2. LOCAL-PERCEPTION

Though patching technique (Cirstea et al., 2022; Nie et al., 2023) has achieved some progress in time series foundation models, its fixed receptive field may limit models' generalization capabilities, thus requiring heavy backbones. The core reason is that the inherent periods and trends within data vary across datasets from distinct domains, causing the diversity of frequencies, but the fixed patch size in pretrained models only captures the same span without considering the changing surrounding environmental information.

Specifically, in pretraining scenarios, a patch with the fixed length may cover the whole period in one pretraining dataset and only covers, e.g., the 70% period in another—see Figure 2(b), which causes burden to understand this semantic transformation. To tackle this limitation, we manage to recognize the varying periods, then align their information with patch-wise tokens to supplement the environmental semantics. First, we adopt the FFT (Brigham & Morrow, 1967) to find the period of the input series:

$$\mathcal{A} = \text{Amp}(\text{FFT}(X)), \mathcal{F} = \arg \max(\mathcal{A}), P = \left\lceil \frac{T}{\mathcal{F}} \right\rceil, \quad (15)$$

where $\text{FFT}(\cdot)$ and $\text{Amp}(\cdot)$ denote the FFT and the calcula-

tion of amplitude values. P is the searched period length. Then we consider the relative positional relations between the patch and the surrounding period to make alignment:

$$s = \lfloor (p + P - 1) / P \rfloor \cdot P - p, \quad (16)$$

$$X' = \text{LeftPadding}(X, s), \quad (17)$$

$$X^{P'} = [w_1, w_2, \dots, w_n], \quad (18)$$

where $X^{P'} \in \mathbb{R}^{n \times (p+s)}$ are the local environmental patches. The padding length s is used to make each local environmental patch $w_i \in \mathbb{R}^{p+s}$ cover the corresponding patch $h_i \in \mathbb{R}^p$, and $p + s$ is the integer multiple of the period P . These operations can help align the intricate and varying local information w_i to the patch h_i .

For each $w_i \in \mathbb{R}^{p+s}$, its length varies with the sample during pretraining due to the multiple frequencies of the time series corpus, which is hard to be encoded through predefined neural networks like MLPs. To overcome this, we propose to utilize the LegT Legendre Memory—see Section 2, to encode the varying local environmental information, i.e., the varying periods, into vectors of the fixed size. For each $w_i \in \mathbb{R}^{p+s}$, we use the discretized form of LegT to compress it like a state space model in an autoregressive manner:

$$\bar{A} = I - (\Delta t / \theta) A, \bar{B} = (\Delta t / \theta) B, \quad (19)$$

$$f_t = w_{i,t}, m_0 = 0, m_t = \bar{A} m_{t-1} + \bar{B} f_t, \quad (20)$$

where $\theta = p + s$ is determined based on the length of w_i , $A \in \mathbb{R}^{d \times d}$ and $B \in \mathbb{R}^{d \times 1}$ are untrainable and initialized

through Formula (4), Δt is a predefined parameter to control the granularity of zero-order hold (ZOH). This mechanism compresses the local environmental patch $w_i \in \mathbb{R}^{p+s}$ with *varying lengths* into the memory cell $m_t \in \mathbb{R}^d$ with the *fixed size*. The generated environmental tokens are:

$$X^{token'} = [w'_1, w'_2, \dots, w'_n], \quad (21)$$

where each token $w'_i \in \mathbb{R}^d$ is the last state of memory cell. We then fuse the original tokens X^{token} and the environmental tokens $X^{token'}$ into $H \in \mathbb{R}^{n \times d}$: $H = X^{token} + X^{token'}$. According to Theorem 2.1, the dimension d is often greater than θ , which helps preserve the full semantics.

3.1.3. MSA-ENCODER

After obtaining the fused tokens, we use the Multi-head Self-Attention Layer as the encoder to generate the hidden representations of them. Through fully-connected interaction, the MSA-Encoder aims at learning the similarities and differences among patterns and environmental information within the tokens:

$$H' = \text{MSA-Encoder}(H), \quad (22)$$

the representations $H' \in \mathbb{R}^{n \times d}$ are the outputs of the Encoding phase, and provide rich semantics within data.

3.2. Decoding

3.2.1. SSD-DECODER

We utilize LegT in Local-Perception of the Encoding phase to enrich the local environmental information. In the Decoding phase, the long-range modeling capability gains more attention, which calls for adaptive memory utilization when making long-term forecasts. Structured State-Space Duality (SSD) Layer or Mamba2 (Dao & Gu, 2024), uses the selective state space modeling mechanism to adaptively process historical information, significantly improving efficiency while achieving similar accuracy to Transformers. Its mechanism takes the form as follows:

$$m_t = A_t m_t + B_t x_t, y_t = C_t^T m_t, \quad (23)$$

where the form shares similarities with LegS, see-Formula (10). Previous works (Gu & Dao, 2023; Dao & Gu, 2024) demonstrate that adapting A, B, C to selective A_t, B_t, C_t can enhance the non-linearity capability. Among them, A_t is obtained from A through the learnable granularity Δt of discretization, so that the initialization of A still matters. To preserve the capability of adaptive memory utilization and ensure the linear complexity of SSD, we use the diagonal of A in LegS—see Formula (12), as the initialization of A_t . We then use the SSD layer with initialized A_t as the Decoder to forecast the future tokens:

$$F = \text{SSD-Decoder}(H'), \quad (24)$$

where $F \in \mathbb{R}^{l \times d}$. Supposing the length of forecasting horizon is L , $l = \lceil L/p \rceil$. Based on the LegS, SSD-Decoder can efficiently memorize all the information from inputs and adaptively utilize them like Transformers.

3.2.2. MCA-ENHANCER

We then use the Multi-head Cross-Attention Layer to further enhance the outputs through recalling the similar representations in the inputs. Specifically, we set F as Query, H' as Key and Value. Through skip connections in MCA-Enhancer, it effectively enhances the F :

$$F' = \text{MCA-Enhancer}(F), \quad (25)$$

where $F' \in \mathbb{R}^{l \times d}$ are the outputs of the Decoding phase, which contain the high-order semantic information obtained from the token transition process in the hidden spaces.

3.3. Flow-based Head

Through pretraining on Time Series Corpus from multiple domains, the Encoding and Decoding phases of FLAME possess strong capability of modeling the token transition principles, which means $F' \in \mathbb{R}^{l \times d}$ are high-quality representations for forecasting. In time series foundation models, making token-wise forecasts through relative lightweight heads can preserve efficiency and ensure the heavy backbones do learn the “knowledge” (Liu et al., 2024c; 2025d).

However, since the inherent temporal causality within time series data, patch-based forecasting models only model the token-wise causal relationships in decoding. When transforming these high-dimension tokens into patch sizes for forecasts, the fine-grained causal relationships within each patch are often neglected. To support generative probabilistic forecasting, keep lightweight, and capture such fine-grained causal relationships, we meticulously devise the couple layers of Normalization Flow to model the intricate probabilistic distributions of real-data. The whole generative process is formulated as:

$$F' = [o_1, o_2, \dots, o_l], \quad (26)$$

$$\epsilon_i \sim \mathcal{N}(0, I), \mathcal{F}_i = \text{Concat}[\epsilon_i, o_i], \quad (27)$$

$$\hat{Y}_i = f_K \circ f_{K-1} \circ \dots \circ f_1(\mathcal{F}_i), \quad (28)$$

where we utilize the tokens $F' = [o_1, o_2, \dots, o_l] \in \mathbb{R}^{l \times d}$ as the prior conditions, and the Gaussian Noise $\epsilon_i \in \mathbb{R}^p$ is the initialization. We concat them to obtain $\mathcal{F}_i \in \mathbb{R}^{p+d}$ as the input of couple layers. The structure of couple layers f_i is the masked MLP:

$$\mathcal{M}_{n,k} = \begin{cases} 0 & \text{if } n < k \leq p \\ 1 & \text{otherwise} \end{cases}, \quad (29)$$

$$\mathcal{F}'_i = f_i(\mathcal{F}_i) = \text{MLP}_{\mathcal{M}}^i(\mathcal{F}_i), \quad (30)$$

where the mask $\mathcal{M} \in \mathbb{R}^{(p+d) \times (p+d)}$ determines the connection pattern of neurons in MLP-based couple layer $f_i := \text{MLP}_{\mathcal{M}}^i$, which determines the interactions among dimensions of $\mathcal{F}_i \in \mathbb{R}^{p+d}$. Considering the output $\mathcal{F}'_i \in \mathbb{R}^{p+d}$, $\mathcal{M}_{n,k} = 0$ indicates that $\mathcal{F}'_i[k]$ cannot see $\mathcal{F}_i[n]$ when calculated in f_i , and vice versa. This means f_i allows the conditional part $o_i \in \mathbb{R}^d$ of \mathcal{F}_i to self-interact and interact with all the dimension of $\epsilon_i \in \mathbb{R}^d$, and works in an autoregressive manner to ensure the noise part $\epsilon_i[j]$ only interacts with $\epsilon_i[\leq j]$ to preserve the fine-grained causal relationships within each patch—see Figure 2(f). Through K coupled layers of generative probabilistic modeling, the final outputs are:

$$\hat{Y} = [\hat{Y}_1, \hat{Y}_2, \dots, \hat{Y}_L], \quad (31)$$

where $\hat{Y} \in \mathbb{R}^{L \times p}$ can be further flattened and fetched the first L points as the forecasts. With the MLP-based couple layers, Flow-based Head can achieve intricate distributional transformation while keeping lightweight. Due to the probabilistic generative mechanism, multiple samplings are recommended to evaluate the forecasted distributions. For clarity, we replace \hat{Y}_i and \mathcal{F}_i with x and z in the token-wise optimization objective:

$$\log p_X(x) = \log p_Z(z) - \sum_{k=1}^K \log \left| \det \left(\frac{\partial f_k(z_{k-1})}{\partial z_{k-1}} \right) \right| \quad (32)$$

4. Experiments

We introduce the detailed experimental settings in Appendix A, and show the zero-shot performance of FLAME in Section 4.1 (deterministic) and Section 4.2 (probabilistic). We also make detailed analysis on key components of FLAME to reveal where the generalization capability comes in Section 4.3. To analyze the scability of FLAME, we make studies on training and inference in Section 4.4. As an important property for deployment, we also analyze the efficiency of FLAME in Section 4.5. In summary—see Figure 3, our proposed FLAME achieves most 1st counts and keeps the most lightweight. We provide all results in Appendix C, including full results of Table 1 and 2, and other results on full-shot settings and short-term forecasting.

4.1. Deterministic Forecasting

As shown in Table 1, the FLAME family consistently outperforms other advanced time series foundation models on datasets from TSFM-Bench. Compared with the recent state-of-the-art models Sundial, FLAME Large outperforms it in most settings, achieving most 1st counts in zero-shot deterministic forecasting tasks. Note that even the FLAME Small (2M) can achieve competitive performance with Sundial Base (128M) while only possessing the $1/64$ parameter

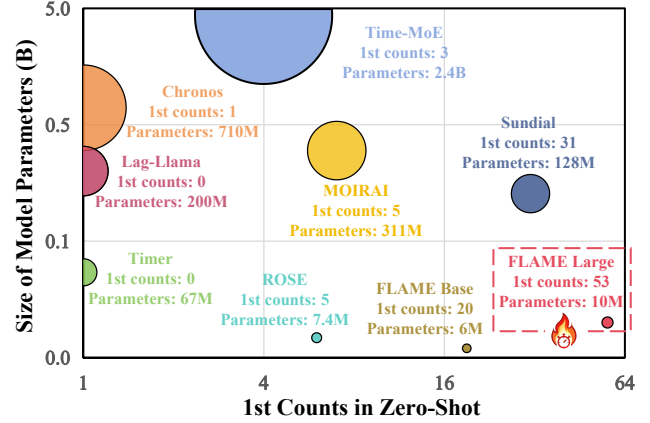


Figure 3. The parameter scale and zero-shot performance of Time Series Foundation models. FLAME Large achieves most 1st counts while keeping the most lightweight.

scale. Compared with the heaviest model Time-MoE Ultra (2.4B), FLAME Small possesses the $1/1,200$ parameter scale but achieves average MSE reduction of 15.0% . Considering lightweight baselines like UniTS and ROSE, FLAME Small also shows excellent advantages in generalization capabilities, achieving significant average MSE reductions of 26.3% and 17.4% .

4.2. Probabilistic Forecasting

Table 2 represents the results of probabilistic forecasting on ProbTS. Among time series foundation models, only FLAME and Sundial adopt generative probabilistic modeling and show excellent advantages over other models. Considering the accuracy, FLAME Large achieves the most 1st counts in zero-shot probabilistic forecasting tasks, excelling both the periodic scenarios like ETT and Weather, and unstationary scenarios like Exchange and ILI. Compared with the previous well-recognized baseline MOIRAI Large and Chronos Large, FLAME Large achieves significant average CRPS reductions of 34.3% and 18.1% , demonstrating the strong capability of modeling intricate distributions over the forecasting horizons. We observe that FLAME’s zero-shot performance can even outperform the full-shot baselines a lot. Compared with diffusion-based CSDI and Flow-based GRU NVP, which need dozens of hours to train from scratch on a large dataset, FLAME Large separately achieves average 23.5% and 35.1% CRPS reduction. This demonstrates the effectiveness of Flow-based head in FLAME, which provides both efficiency and accuracy.

4.3. Model Analysis

To reveal where the generalization capability of FLAME comes, we analyze the key components of FLAME including Local-Perception, SSD-Decoder, and Flow-based Head in Table 3. Results show that all of our designs are the most reasonable, see—Appendix B for full results and analytics.

Table 1. Average results of zero-shot deterministic forecasting experiments on datasets from TSFM-Bench. Lower MSE or MAE values indicate better predictions. ('-') denotes datasets included in the model’s pretraining and therefore excluded from testing. **Red**: the best, **Blue**: the 2nd best. All the results are listed in Table 13 of Appendix C.

Models	FLAME Small		FLAME Base		FLAME Large		Sundial (2025)		LightGTS (2025)		ROSE (2025)		Timer (2024)		Chronos (2024)		Time-MoE (2024)		TinyTTM (2024)		MOIRAI (2024)		
	MSE	MAE	MSE	MAE	MSE	MAE	MSE	MAE	MSE	MAE	MSE	MAE	MSE	MAE	MSE	MAE	MSE	MAE	MSE	MAE	MSE	MAE	
ETT (Avg)	0.339	0.382	<u>0.339</u>	0.381	0.344	0.385	0.335	<u>0.379</u>	0.339	0.379	0.393	0.411	0.551	0.478	0.442	0.408	0.357	0.390	0.441	0.430	0.382	0.388	
Weather	0.215	0.261	0.222	0.269	0.227	0.273	0.234	0.270	<u>0.219</u>	<u>0.267</u>	0.265	0.305	0.292	0.313	0.288	0.309	0.256	0.289	0.265	0.307	0.260	0.275	
Electricity	0.287	0.371	0.222	0.319	<u>0.217</u>	<u>0.313</u>	0.169	0.265	0.233	0.319	0.234	0.320	0.297	0.375	-	-	-	-	0.222	0.317	0.188	0.273	
Traffic	0.673	0.461	0.576	0.396	0.546	0.384	-	-	0.610	0.399	0.588	0.412	0.613	0.407	0.615	0.421	-	-	-	<u>0.564</u>	<u>0.386</u>	-	-
Solar	0.203	0.278	<u>0.184</u>	0.277	0.168	<u>0.272</u>	0.221	0.252	0.219	0.305	0.505	0.549	0.771	0.604	0.393	0.319	0.411	0.428	0.815	0.710	0.714	0.704	
PEMS08	0.324	0.384	<u>0.312</u>	<u>0.374</u>	0.293	0.351	-	-	0.812	0.692	1.369	0.979	0.866	0.695	1.707	1.024	-	-	1.730	1.066	-	-	
Wind	1.144	0.765	<u>1.120</u>	<u>0.758</u>	1.042	0.733	1.186	0.772	1.292	0.836	1.251	0.820	1.201	0.783	1.478	0.834	-	-	1.337	0.829	1.299	0.795	
NYSE	<u>0.527</u>	0.553	0.442	0.430	0.529	<u>0.507</u>	0.880	0.642	0.620	0.626	-	-	0.988	0.704	1.129	0.720	-	-	-	-	0.492	0.441	
1 st Count	8	8	6	4	15	9	<u>9</u>	<u>9</u>	0	3	3	2	0	0	0	0	1	2	2	3	0	4	
2 nd Count	3	1	15	<u>9</u>	2	10	2	7	<u>9</u>	6	2	3	0	0	0	0	2	1	5	3	4	4	

Table 2. Average results of zero-shot probabilistic forecasting experiments on datasets from ProbTS. Lower CRPS or NMAE values indicate better predictions. ('-') denotes datasets included in the model’s pretraining and therefore excluded from testing. ('/') denotes the excessive time consumption. **Red**: the best, **Blue**: the 2nd best. Full results are in Table 14 of Appendix C.

Models	FLAME Small		FLAME Base		FLAME Large		Sundial (2025)		Chronos (2024)		MOIRAI (2024)		Lag-Llama (2023)		TSDiff (2023)		CSDI (2022)		TimeGrad (2022)		GRU NVP (2021)	
	CRPS	NMAE	CRPS	NMAE	CRPS	NMAE	CRPS	NMAE	CRPS	NMAE	CRPS	NMAE	CRPS	NMAE	CRPS	NMAE	CRPS	NMAE	CRPS	NMAE	CRPS	NMAE
ETT (Avg)	<u>0.235</u>	<u>0.293</u>	0.250	0.317	0.236	0.295	0.231	0.273	0.290	0.316	0.366	0.377	0.273	0.310	0.370	0.465	0.304	0.389	0.493	0.619	0.476	0.605
Weather	0.089	0.114	<u>0.087</u>	0.105	0.074	0.090	0.087	<u>0.102</u>	0.142	0.158	0.179	0.143	0.096	0.106	0.132	0.134	0.077	0.093	0.125	0.155	0.119	0.147
Electricity	0.093	0.118	0.086	0.110	0.081	0.097	<u>0.081</u>	<u>0.098</u>	-	-	0.247	0.290	-	-	0.407	0.519	/	/	0.102	0.126	0.101	0.127
Traffic	0.268	0.337	<u>0.248</u>	0.306	0.247	<u>0.308</u>	-	-	0.269	0.295	-	-	0.330	0.385	0.327	0.392	/	/	0.211	0.246	0.198	0.245
Exchange	0.043	0.048	0.040	0.047	<u>0.042</u>	<u>0.047</u>	0.045	0.049	0.044	0.047	0.045	0.050	0.057	0.069	0.084	0.111	0.069	0.086	0.082	0.095	0.073	0.093
ILI	0.162	0.198	0.130	0.166	0.154	0.188	<u>0.148</u>	<u>0.166</u>	0.170	0.197	0.159	0.197	0.156	0.211	0.248	0.259	0.276	0.290	0.284	0.310	0.283	0.309
1 st Count	3	3	5	3	15	14	5	<u>8</u>	0	1	0	1	0	0	0	0	2	2	0	2	4	2
2 nd Count	<u>7</u>	5	<u>7</u>	5	7	6	5	8	0	2	1	1	1	0	0	0	6	5	4	2	0	2

Table 3. Ablation studies on Local-Perception (line 3-5), SSD-Decoder (line 6-8), and Flow-based Head (line 9-11). We choose ETT (Avg), Weather, Electricity and Traffic (shared in TSFM-Bench and ProbTS), and report average MSE and CRPS to evaluate deterministic and probabilistic forecasting.

Variants	ETT (Avg)		Weather		Electricity		Traffic	
	MSE	CRPS	MSE	CRPS	MSE	CRPS	MSE	CRPS
w/o Local-Perception	0.374	0.266	0.278	0.104	0.293	0.109	0.690	0.283
w/o Period Alignment	0.368	0.251	0.248	0.083	0.275	0.096	0.627	0.264
Learnable LegT	<u>0.348</u>	<u>0.245</u>	<u>0.237</u>	<u>0.074</u>	<u>0.222</u>	<u>0.084</u>	<u>0.566</u>	<u>0.253</u>
Self-Attention Decoder	0.391	0.300	<u>0.253</u>	0.106	0.300	0.131	0.654	0.341
Causal-Attention Decoder	0.369	0.260	0.255	0.103	0.230	0.095	0.560	<u>0.266</u>
Mamba v1 Decoder	<u>0.362</u>	<u>0.254</u>	0.256	<u>0.098</u>	<u>0.218</u>	<u>0.087</u>	<u>0.557</u>	0.277
VAE Head	0.366	0.262	0.264	0.093	0.291	0.138	0.745	0.506
Diffusion Head	0.360	0.252	<u>0.230</u>	<u>0.077</u>	0.235	0.088	<u>0.568</u>	<u>0.266</u>
Flow Match Head	<u>0.358</u>	<u>0.251</u>	0.233	0.080	<u>0.232</u>	<u>0.088</u>	0.595	0.297
FLAME Large	0.344	0.236	0.227	0.074	0.217	0.081	0.546	0.247

4.4. Scability Analysis

Though the FLAME family possesses extremely lightweight backbones while achieving state-of-the-art performance, we reveal that it also possesses the potential of scability. As shown in Figure 4, the training curves of the FLAME family indicate that the model capacity increases with the parameter scale. According to the results in Table 1–2, the zero-shot performance also gets better and the FLAME Large achieves most 1st Counts in both deterministic and probabilistic forecasting tasks.

Since FLAME models distributions over the forecasting horizon, we also study the scability of generative forecasting

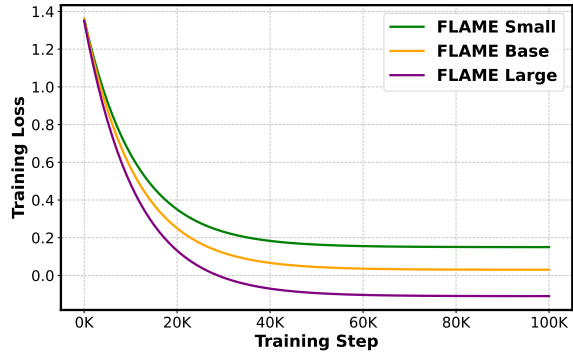


Figure 4. The training curves of the FLAME family.

by exploring the correlations between the sampling number and performance—see Figure 5. The results show that the CPRS and NMAE keep consistent promotion as the sampling number increases, and achieve good performance in the number of 100, which may not cause large efficiency burdens in real-world applications.

4.5. Efficiency Analysis

As a characteristic property of FLAME, the extreme efficiency owes to the lightweight backbone and Flow-based Head. For detailed quantification, we report the Parameter scale, Multiply-Accumulate Operations (MACs), Max GPU Memory Occupation, and Inference Time in Table 4. We

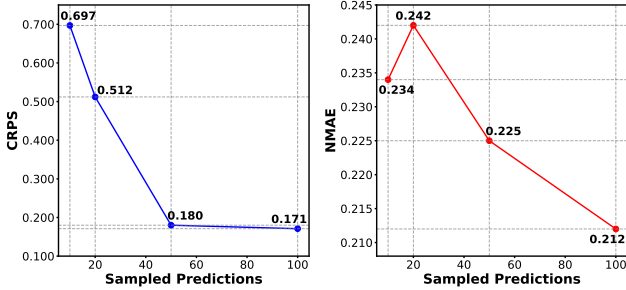


Figure 5. We show the CRPS and NMAE on ProbTS w.r.t. the sampling number. Full results are in Table 9 of Appendix B.

compare the FLAME Large with time series foundation models and end-to-end supervised probabilistic models.

Results show FLAME Large achieves consistent efficiency advantages over other time series foundation models. Compared with end-to-end supervised models like TimeGrad and CSDI, FLAME Large also has less parameters, faster inference speed, and less MACs and GPU Memory.

Table 4. Efficiency analysis of FLAME and other baselines on ETTm1 dataset, evaluated with the horizon of 720 and batch size of 1. We report the Parameter scale, MACs, Max GPU Memory, and Inference Time.

Models	Parameters	MACs	GPU (MB)	Inference (s)
Timer	67.4 M	52.6 G	1,435	0.08
TimesFM	200 M	624.9 G	1,395	0.16
Chronos Large	700 M	92327.9 G	10,269	34.33
MOIRAI Large	300 M	97.36 G	2,009	0.1
Time-MoE Ultra	453 M	5252.9 G	14,131	2.13
Sundial Base	128 M	432.3 G	603	0.1
TimeGrad	12.3 M	19.3 G	522	28.61
CSDI	15.9 M	37.5 G	817	86.18
FLAME Large	10.6 M	0.238 G	129	0.037

5. Related works

5.1. Time Series Forecasting

Deterministic Time Series Forecasting is critical in decision intelligence, which has facilitated a surge of modern deep learning methods like PatchTST (Nie et al., 2023), Pathformer (Chen et al., 2024b), and DUET (Qiu et al., 2025e). LMU (Voelker et al., 2019) and FiLM (Zhou et al., 2022) first introduce Legendre Memory (LegT) in time series forecasting but they consider compressing the whole input series into state vectors, which may cause the information loss. Compared with them, FLAME leverages the LegT in compressing varying token-wise environmental information and aligning them with the original tokens, thus adapting to the multiple frequencies in pretraining corpus and obtaining strong generalization capabilities. Another important direction is Probabilistic Time Series Forecasting, which can quantify the uncertainties and produce more practical significance in real-world applications. Recently,

generative mechanisms such as VAE, Diffusion, and Flow are widely studied. Among them, D^3 VAE (Li et al., 2022) and K^2 VAE (Wu et al., 2025b) are the most advanced VAE models in probabilistic time series forecasting. Considering multi-step generative mechanisms like Diffusion and Normalization Flow, recent models include GRU NVP (Rasul et al., 2021b), CSDI (Tashiro et al., 2021), TimeGrad (Rasul et al., 2021a), and TSDiff (Kollovieh et al., 2023), showing strong performance. Compared with them, FLAME is the first foundation model to adapt normalization flow for token-wise probabilistic modeling.

5.2. Time Series Foundation Models

Recent studies on Time Series Foundation Models manage to reveal the source of generalization capability. Distinct Transformer-based architectures are devised and heavily stacked, and are trained on billion- or trillion-scale time series corpus, to make efforts in capturing the inherent inductive bias within data. Among them, TimesFM (Das et al., 2024), Timer (Liu et al., 2024c), and Time-MoE (Shi et al., 2024) are strong deterministic forecasting baselines, with heavy backbones and strong zero-shot performance. However, works like UniTS (Gao et al., 2024), TinyTTM (Ekambaram et al., 2024), ROSE (Wang et al., 2025c) also demonstrate that light backbones can also achieve state-of-the-art deterministic forecasting performance if the inductive bias is captured in a more efficient way. Some time series foundation models support probabilistic forecasting, among them, Lag-Llama (Rasul et al., 2023), Chronos (Ansari et al.), Moirai (Woo et al., 2024), and Sundial (Liu et al., 2025d) have outperformed some end-to-end supervised probabilistic models. However, all of them possess heavy backbones with hundreds-million to billion parameters, which are not very efficient in making generative probabilistic forecasts on large downstream datasets. Moreover, no existing methods explore how to achieve outstanding probabilistic forecasting performance with lightweight architectures. In this paper, we propose FLAME to handle this bottleneck.

6. Conclusion

In this work, we propose a family of extremely lightweight and highly capable time series foundation models, named FLAME. To sum up, FLAME adapts the Legendre Memory in the backbone to compress varying local environmental information into time series tokens and support adaptive memory utilization in long-range forecasting, thus obtaining strong generalization capabilities. FLAME also supports probabilistic time series forecasting through a Normalization Flow based forecasting head. Comprehensive experiments on deterministic and probabilistic forecasting tasks demonstrate that FLAMEs are strong out-of-the-box tools of decision intelligence, possessing both accuracy and effi-

ciency.

In the future work, we will further explore the non-deterministic modeling in all the tasks of time series analysis, e.g., probabilistic imputation, time series generation, anomaly detection, and classification. Another direction is to develop more lightweight and robust mechanisms to support generative modeling, and extend them via pretraining to the out-of-the-box paradigm.

References

- Achiam, J., Adler, S., Agarwal, S., Ahmad, L., Akkaya, I., Aleman, F. L., Almeida, D., Altenschmidt, J., Altman, S., Anadkat, S., et al. Gpt-4 technical report. *arXiv preprint arXiv:2303.08774*, 2023.
- Ansari, A. F., Stella, L., Turkmen, A. C., Zhang, X., Mercado, P., Shen, H., Shchur, O., Rangapuram, S. S., Arango, S. P., Kapoor, S., et al. Chronos: Learning the language of time series. *Transactions on Machine Learning Research*.
- Bagnall, A., Dau, H. A., Lines, J., Flynn, M., Large, J., Bostrom, A., Southam, P., and Keogh, E. The uea multivariate time series classification archive, 2018. *arXiv preprint arXiv:1811.00075*, 2018.
- Box, G. E. and Pierce, D. A. Distribution of residual autocorrelations in autoregressive-integrated moving average time series models. *Journal of the American statistical Association*, 65(332):1509–1526, 1970.
- Brigham, E. O. and Morrow, R. The fast fourier transform. *IEEE spectrum*, 4(12):63–70, 1967.
- Chen, M., Shen, L., Li, Z., Wang, X. J., Sun, J., and Liu, C. Visionts: Visual masked autoencoders are free-lunch zero-shot time series forecasters. *arXiv preprint arXiv:2408.17253*, 2024a.
- Chen, P., Zhang, Y., Cheng, Y., Shu, Y., Wang, Y., Wen, Q., Yang, B., and Guo, C. Pathformer: Multi-scale transformers with adaptive pathways for time series forecasting. In *ICLR*, 2024b.
- Cirstea, R., Guo, C., Yang, B., Kieu, T., Dong, X., and Pan, S. Triformer: Triangular, variable-specific attentions for long sequence multivariate time series forecasting. In *IJCAI*, pp. 1994–2001, 2022.
- Dai, T., Wu, B., Liu, P., Li, N., Bao, J., Jiang, Y., and Xia, S.-T. Periodicity decoupling framework for long-term series forecasting. In *ICLR*, 2024a.
- Dai, T., Wu, B., Liu, P., Li, N., Bao, J., Jiang, Y., and Xia, S.-T. Periodicity decoupling framework for long-term series forecasting. In *ICLR*, 2024b.
- Dai, T., Wu, B., Liu, P., Li, N., Yuerong, X., Xia, S.-T., and Zhu, Z. Ddn: Dual-domain dynamic normalization for non-stationary time series forecasting. In *NeurIPS*, 2024c.
- Dao, T. and Gu, A. Transformers are ssms: Generalized models and efficient algorithms through structured state space duality. *arXiv preprint arXiv:2405.21060*, 2024.
- Das, A., Kong, W., Sen, R., and Zhou, Y. A decoder-only foundation model for time-series forecasting. In *Forty-first International Conference on Machine Learning*, 2024.
- Dau, H. A., Bagnall, A., Kamgar, K., Yeh, C.-C. M., Zhu, Y., Gharghabi, S., Ratanamahatana, C. A., and Keogh, E. The ucr time series archive. *IEEE/CAA Journal of Automatica Sinica*, 6(6):1293–1305, 2019.
- Durkan, C., Bekasov, A., Murray, I., and Papamakarios, G. Neural spline flows. *Advances in neural information processing systems*, 32, 2019.
- Ekambaram, V., Jati, A., Dayama, P., Mukherjee, S., Nguyen, N., Gifford, W. M., Reddy, C., and Kalagnanam, J. Tiny time mixers (ttms): Fast pre-trained models for enhanced zero/few-shot forecasting of multivariate time series. *Advances in Neural Information Processing Systems*, 37:74147–74181, 2024.
- Gao, S., Koker, T., Queen, O., Hartvigsen, T., Tsiligkaridis, T., and Zitnik, M. Units: Building a unified time series model. *arXiv*, 2024. URL <https://arxiv.org/pdf/2403.00131.pdf>.
- Godaheva, R., Bergmeir, C., Webb, G. I., Hyndman, R. J., and Montero-Manso, P. Monash time series forecasting archive. *arXiv preprint arXiv:2105.06643*, 2021a.
- Godaheva, R., Bergmeir, C., Webb, G. I., Hyndman, R. J., and Montero-Manso, P. Monash time series forecasting archive. *arXiv preprint arXiv:2105.06643*, 2021b.
- Gu, A. and Dao, T. Mamba: Linear-time sequence modeling with selective state spaces. *arXiv preprint arXiv:2312.00752*, 2023.
- Gu, A., Dao, T., Ermon, S., Rudra, A., and Ré, C. Hippo: Recurrent memory with optimal polynomial projections. *Advances in neural information processing systems*, 33: 1474–1487, 2020.
- Hu, Y., Liu, P., Zhu, P., Cheng, D., and Dai, T. Adaptive multi-scale decomposition framework for time series forecasting. In *AAAI*, 2025a.
- Hu, Y., Zhang, G., Liu, P., Lan, D., Li, N., Cheng, D., Dai, T., Xia, S.-T., and Pan, S. Timefilter: Patch-specific

- spatial-temporal graph filtration for time series forecasting. *ICML*, 2025b.
- Jin, M., Wang, S., Ma, L., Chu, Z., Zhang, J. Y., Shi, X., Chen, P.-Y., Liang, Y., Li, Y.-F., Pan, S., and Wen, Q. Time-LLM: Time series forecasting by reprogramming large language models. In *International Conference on Learning Representations (ICLR)*, 2024.
- Khan, S., Naseer, M., Hayat, M., Zamir, S. W., Khan, F. S., and Shah, M. Transformers in vision: A survey. *ACM computing surveys (CSUR)*, 54(10s):1–41, 2022.
- Kim, T., Kim, J., Tae, Y., Park, C., Choi, J.-H., and Choo, J. Reversible instance normalization for accurate time-series forecasting against distribution shift. In *ICLR*, 2021.
- Kollovich, M., Ansari, A. F., Bohlke-Schneider, M., Zschiegner, J., Wang, H., and Wang, Y. Predict, refine, synthesize: Self-guiding diffusion models for probabilistic time series forecasting. In *NeurIPS*, 2023.
- Li, L., Lu, S., Ren, Y., and Kong, A. W.-K. Set you straight: Auto-steering denoising trajectories to sidestep unwanted concepts. *arXiv preprint arXiv:2504.12782*, 2025a.
- Li, X., He, Y., Zu, S., Li, Z., Shi, T., Xie, Y., and Zhang, K. Multi-modal large language model with rag strategies in soccer commentary generation. In *WACV*, pp. 6197–6206, 2025b.
- Li, Y., Yu, R., Shahabi, C., and Liu, Y. Diffusion convolutional recurrent neural network: Data-driven traffic forecasting. *arXiv preprint arXiv:1707.01926*, 2017.
- Li, Y., Lu, X., Wang, Y., and Dou, D. Generative time series forecasting with diffusion, denoise, and disentanglement. *Advances in Neural Information Processing Systems*, 35: 23009–23022, 2022.
- Li, Z., Qiu, X., Chen, P., Wang, Y., Cheng, H., Shu, Y., Hu, J., Guo, C., Zhou, A., Jensen, C. S., and Yang, B. TSFM-Bench: Comprehensive and unified benchmarking of foundation models for time series forecasting. In *SIGKDD*, 2025c.
- Lin, S., Lin, W., Wu, W., Zhao, F., Mo, R., and Zhang, H. Segrnn: Segment recurrent neural network for long-term time series forecasting. *arXiv preprint arXiv:2308.11200*, 2023.
- Liu, A., Feng, B., Xue, B., Wang, B., Wu, B., Lu, C., Zhao, C., Deng, C., Zhang, C., Ruan, C., et al. Deepseek-v3 technical report. *arXiv preprint arXiv:2412.19437*, 2024a.
- Liu, M., Zeng, A., Chen, M., Xu, Z., Lai, Q., Ma, L., and Xu, Q. Scinet: Time series modeling and forecasting with sample convolution and interaction. *NeurIPS*, 35: 5816–5828, 2022.
- Liu, P., Guo, H., Dai, T., Li, N., Bao, J., Ren, X., Jiang, Y., and Xia, S.-T. Calf: Aligning llms for time series forecasting via cross-modal fine-tuning. *AAAI*, 39(18): 18915–18923, 2025a.
- Liu, P., Wu, B., Hu, Y., Li, N., Dai, T., Bao, J., and Xia, S.-T. Timebridge: Non-stationarity matters for long-term time series forecasting. In *ICML*, 2025b.
- Liu, X., Qiu, X., Wu, X., Li, Z., Guo, C., Hu, J., and Yang, B. Rethinking irregular time series forecasting: A simple yet effective baseline. *arXiv preprint arXiv:2505.11250*, 2025c.
- Liu, X., Qiu, X., Wu, X., Li, Z., Guo, C., Hu, J., and Yang, B. Rethinking irregular time series forecasting: A simple yet effective baseline. In *AAAI*, 2026.
- Liu, Y., Hu, T., Zhang, H., Wu, H., Wang, S., Ma, L., and Long, M. itransformer: Inverted transformers are effective for time series forecasting. In *ICLR*, 2024b.
- Liu, Y., Zhang, H., Li, C., Huang, X., Wang, J., and Long, M. Timer: Generative pre-trained transformers are large time series models. In *International Conference on Machine Learning*, pp. 32369–32399. PMLR, 2024c.
- Liu, Y., Qin, G., Shi, Z., Chen, Z., Yang, C., Huang, X., Wang, J., and Long, M. Sundial: A family of highly capable time series foundation models. *arXiv preprint arXiv:2502.00816*, 2025d.
- Liu, Z., Lin, Y., Cao, Y., Hu, H., Wei, Y., Zhang, Z., Lin, S., and Guo, B. Swin transformer: Hierarchical vision transformer using shifted windows. In *Proceedings of the IEEE/CVF international conference on computer vision*, pp. 10012–10022, 2021.
- Lu, S., Liu, Y., and Kong, A. W.-K. Tf-icon: Diffusion-based training-free cross-domain image composition. In *ICCV*, pp. 2294–2305, 2023.
- Lu, S., Wang, Z., Li, L., Liu, Y., and Kong, A. W.-K. Mace: Mass concept erasure in diffusion models. In *CVPR*, pp. 6430–6440, 2024a.
- Lu, S., Zhou, Z., Lu, J., Zhu, Y., and Kong, A. W.-K. Robust watermarking using generative priors against image editing: From benchmarking to advances. *arXiv preprint arXiv:2410.18775*, 2024b.
- McCracken, M. W. and Ng, S. Fred-md: A monthly database for macroeconomic research. *Journal of Business & Economic Statistics*, 34(4):574–589, 2016.

- Nie, Y., Nguyen, N. H., Sinthong, P., and Kalagnanam, J. A time series is worth 64 words: Long-term forecasting with transformers. In *ICLR*, 2023.
- Niu, W., Xie, Z., Sun, Y., He, W., Xu, M., and Hao, C. Langtime: A language-guided unified model for time series forecasting with proximal policy optimization. In *ICML*, 2025.
- Padé, H. Sur la représentation approchée d’une fonction par des fractions rationnelles. In *Annales scientifiques de l’Ecole normale supérieure*, volume 9, pp. 3–93, 1892.
- Pan, Z., Wang, Y., Zhang, Y., Yang, S. B., Cheng, Y., Chen, P., Guo, C., Wen, Q., Tian, X., Dou, Y., et al. MagicScaler: Uncertainty-aware, predictive autoscaling. In *Proc. VLDB Endow.*, 2023.
- Paszke, A., Gross, S., Massa, F., Lerer, A., Bradbury, J., Chanan, G., Killeen, T., Lin, Z., Gimelshein, N., Antiga, L., Desmaison, A., Köpf, A., Yang, E. Z., DeVito, Z., Raison, M., Tejani, A., Chilamkurthy, S., Steiner, B., Fang, L., Bai, J., and Chintala, S. Pytorch: An imperative style, high-performance deep learning library. In *NeurIPS*, pp. 8024–8035, 2019.
- Qiu, X., Hu, J., Zhou, L., Wu, X., Du, J., Zhang, B., Guo, C., Zhou, A., Jensen, C. S., Sheng, Z., and Yang, B. TFB: towards comprehensive and fair benchmarking of time series forecasting methods. *Proc. VLDB Endow.*, 17(9): 2363–2377, 2024.
- Qiu, X., Cheng, H., Wu, X., Hu, J., and Guo, C. A comprehensive survey of deep learning for multivariate time series forecasting: A channel strategy perspective. *arXiv preprint arXiv:2502.10721*, 2025a.
- Qiu, X., Li, X., Pang, R., Pan, Z., Wu, X., Yang, L., Hu, J., Shu, Y., Lu, X., Yang, C., Guo, C., Zhou, A., Jensen, C. S., and Yang, B. Easytime: Time series forecasting made easy. In *ICDE*, 2025b.
- Qiu, X., Li, Z., Qiu, W., Hu, S., Zhou, L., Wu, X., Li, Z., Guo, C., Zhou, A., Sheng, Z., Hu, J., Jensen, C. S., and Yang, B. TAB: Unified benchmarking of time series anomaly detection methods. In *Proc. VLDB Endow.*, 2025c.
- Qiu, X., Wu, X., Cheng, H., Liu, X., Guo, C., Hu, J., and Yang, B. Dbloss: Decomposition-based loss function for time series forecasting. In *NeurIPS*, 2025d.
- Qiu, X., Wu, X., Lin, Y., Guo, C., Hu, J., and Yang, B. DUET: Dual clustering enhanced multivariate time series forecasting. In *SIGKDD*, pp. 1185–1196, 2025e.
- Qiu, X., Zhu, Y., Li, Z., Cheng, H., Wu, X., Guo, C., Yang, B., and Hu, J. Dag: A dual causal network for time series forecasting with exogenous variables. *arXiv preprint arXiv:2509.14933*, 2025f.
- Rasul, K., Seward, C., Schuster, I., and Vollgraf, R. Autoregressive denoising diffusion models for multivariate probabilistic time series forecasting. In *ICML*, volume 139, pp. 8857–8868, 2021a.
- Rasul, K., Sheikh, A., Schuster, I., Bergmann, U. M., and Vollgraf, R. Multivariate probabilistic time series forecasting via conditioned normalizing flows. In *ICLR*, 2021b.
- Rasul, K., Ashok, A., Williams, A. R., Khorasani, A., Adamopoulos, G., Bhagwatkar, R., Biloš, M., Ghonia, H., Hassen, N., Schneider, A., et al. Lag-llama: Towards foundation models for time series forecasting. In *RO-FoMo: Robustness of Few-shot and Zero-shot Learning in Large Foundation Models*, 2023.
- Richard, J.-P. Time-delay systems: an overview of some recent advances and open problems. *automatica*, 39(10): 1667–1694, 2003.
- Shi, X., Wang, S., Nie, Y., Li, D., Ye, Z., Wen, Q., and Jin, M. Time-moe: Billion-scale time series foundation models with mixture of experts. *arXiv e-prints*, pp. arXiv–2409, 2024.
- Sun, Y., Xie, Z., Chen, D., Eldele, E., and Hu, Q. Hierarchical classification auxiliary network for time series forecasting. In *AAAI*, volume 39, pp. 20743–20751, 2025a.
- Sun, Y., Xie, Z., Xing, H., Yu, H., and Hu, Q. Ppgf: Probability pattern-guided time series forecasting. *IEEE Transactions on Neural Networks and Learning Systems*, 2025b.
- Taieb, S. B., Bontempi, G., Atiya, A. F., and Sorjamaa, A. A review and comparison of strategies for multi-step ahead time series forecasting based on the nn5 forecasting competition. *Expert systems with applications*, 39(8): 7067–7083, 2012.
- Tashiro, Y., Song, J., Song, Y., and Ermon, S. CSDI: conditional score-based diffusion models for probabilistic time series imputation. In *NeurIPS*, pp. 24804–24816, 2021.
- Ulyanov, D., Vedaldi, A., and Lempitsky, V. Instance normalization: The missing ingredient for fast stylization. *arXiv preprint arXiv:1607.08022*, 2016.
- Voelker, A., Kajić, I., and Eliasmith, C. Legendre memory units: Continuous-time representation in recurrent neural networks. *Advances in neural information processing systems*, 32, 2019.
- Voelker, A. R. Dynamical systems in spiking neuromorphic hardware. 2019.

- Wang, R., He, Y., Sun, T., Li, X., and Shi, T. Unitmge: Uniform text-motion generation and editing model via diffusion. In *WACV*, pp. 6104–6114, 2025a.
- Wang, Y., Han, Y., Wang, H., and Zhang, X. Contrast everything: A hierarchical contrastive framework for medical time-series. *NeurIPS*, 36, 2024.
- Wang, Y., Qiu, Y., Shu, Y., Rao, Z., Pan, L., Yang, B., and Chenjuan, G. Lightgts: A lightweight general time series forecasting model. In *ICML*, 2025b.
- Wang, Y., Qiu, Y., Zhao, k., Shu, Y., Rao, Z., Pan, L., Yang, B., and Chenjuan, G. Towards a general time series forecasting model with unified representation and adaptive transfer. In *ICML*, 2025c.
- Woo, G., Liu, C., Kumar, A., Xiong, C., Savarese, S., and Sahoo, D. Unified training of universal time series forecasting transformers. In *Forty-first International Conference on Machine Learning*, 2024.
- Wu, H., Hu, T., Liu, Y., Zhou, H., Wang, J., and Long, M. Timesnet: Temporal 2d-variation modeling for general time series analysis. In *ICLR*, 2023.
- Wu, X., Wu, X., Yang, B., Zhou, L., Guo, C., Qiu, X., Hu, J., Sheng, Z., and Jensen, C. S. AutoCTS++: zero-shot joint neural architecture and hyperparameter search for correlated time series forecasting. *VLDB J.*, 33(5): 1743–1770, 2024.
- Wu, X., Qiu, X., Cheng, H., Li, Z., Hu, J., Guo, C., and Yang, B. Enhancing time series forecasting through selective representation spaces: A patch perspective. In *NeurIPS*, 2025a.
- Wu, X., Qiu, X., Gao, H., Hu, J., Yang, B., and Guo, C. K²VAE: A koopman-kalman enhanced variational autoencoder for probabilistic time series forecasting. In *ICML*, 2025b.
- Wu, X., Qiu, X., Li, Z., Wang, Y., Hu, J., Guo, C., Xiong, H., and Yang, B. CATCH: Channel-aware multivariate time series anomaly detection via frequency patching. In *ICLR*, 2025c.
- Wu, X., Wu, X., Zhang, D., Zhang, M., Guo, C., Yang, B., and Jensen, C. S. Fully automated correlated time series forecasting in minutes. In *Proc. VLDB Endow.*, volume 18, pp. 144–157, 2025d.
- Yang, C., He, Y., Tian, A. X., Chen, D., Wang, J., Shi, T., Heydarian, A., and Liu, P. Wcdt: World-centric diffusion transformer for traffic scene generation. *arXiv preprint arXiv:2404.02082*, 2024.
- Yu, C., Wang, F., Shao, Z., Sun, T., Wu, L., and Xu, Y. Ds-former: A double sampling transformer for multivariate time series long-term prediction. In *CIKM*, pp. 3062–3072, 2023.
- Zeng, A., Chen, M., Zhang, L., and Xu, Q. Are transformers effective for time series forecasting? In *AAAI*, volume 37, pp. 11121–11128, 2023.
- Zhang, B., Kieu, T., Qiu, X., Guo, C., Hu, J., Zhou, A., Jensen, C. S., and Yang, B. An encode-then-decompose approach to unsupervised time series anomaly detection on contaminated training data—extended version. *arXiv preprint arXiv:2510.18998*, 2025.
- Zhang, J., Wen, X., Zhang, Z., Zheng, S., Li, J., and Bian, J. ProbTS: Benchmarking point and distributional forecasting across diverse prediction horizons. In *NeurIPS*, 2024.
- Zhang, S., Guo, B., Dong, A., He, J., Xu, Z., and Chen, S. X. Cautionary tales on air-quality improvement in beijing. *Proceedings of the Royal Society A: Mathematical, Physical and Engineering Sciences*, 473(2205):20170457, 2017.
- Zhou, H., Zhang, S., Peng, J., Zhang, S., Li, J., Xiong, H., and Zhang, W. Informer: Beyond efficient transformer for long sequence time-series forecasting. In *AAAI*, volume 35, pp. 11106–11115, 2021.
- Zhou, T., Ma, Z., Wen, Q., Sun, L., Yao, T., Yin, W., Jin, R., et al. Film: Frequency improved legendre memory model for long-term time series forecasting. *Advances in Neural Information Processing Systems*, 35:12677–12690, 2022.
- Zhou, T., Niu, P., Wang, X., Sun, L., and Jin, R. One Fits All: Power general time series analysis by pretrained lm. In *NeurIPS*, 2023.
- Zhou, Y., He, Y., Su, Y., Han, S., Jang, J., Bertasius, G., Bansal, M., and Yao, H. Reagent-v: A reward-driven multi-agent framework for video understanding. *arXiv preprint arXiv:2506.01300*, 2025.

A. Implementation Details

A.1. Pretraining Corpus

To pre-train our model, we utilize a broad collection of time series datasets drawn from multiple sources, including selected subsets from the Monash (Godahehwa et al., 2021b), UEA (Bagnall et al., 2018), and UCR (Dau et al., 2019) repositories, along with several widely-used benchmarks (Zhang et al., 2017; Wang et al., 2024; Liu et al., 2022; McCracken & Ng, 2016; Taieb et al., 2012). A full inventory of these datasets is provided in Table 5. We ensure that none of the pre-training datasets overlap with those used in downstream evaluations. It’s also worth noting that although both the pre-training and target sets include weather data, the former is univariate while the latter contains multivariate sequences. We categorize the pre-training datasets into six domain-specific groups: Energy, Nature, Health, Transport, and Web. These datasets vary significantly in sampling rates, ranging from milliseconds to monthly intervals, capturing the diversity and richness of real-world time series. All datasets are decomposed into univariate sequences and FLAME is trained using a Channel Independent (CI) strategy.

Table 5. List of pretraining datasets.

Domain	Dataset	Frequency	Piont Number	Source
Energy	Aus. Electricity Demand	Half Hourly	1155264	Monash (Godahehwa et al., 2021b)
	Wind	4 Seconds	7397147	Monash (Godahehwa et al., 2021b)
	Wind Farms	Minutely	172178060	Monash (Godahehwa et al., 2021b)
	Solar Power	4 Seconds	7397222	Monash (Godahehwa et al., 2021b)
	London Smart Meters	Half Hourly	166527216	Monash (Godahehwa et al., 2021b)
Economic	FRED_MD	Monthly	77896	(McCracken & Ng, 2016)
	Bitcoin	Daily	75364	Monash (Godahehwa et al., 2021b)
	NN5	Daily	87801	(Taieb et al., 2012)
Health	MotorImagery	0.001 Seconds	72576000	UEA (Bagnall et al., 2018)
	SelfRegulationSCP1	0.004 Seconds	3015936	UEA (Bagnall et al., 2018)
	SelfRegulationSCP2	0.004 Seconds	3064320	UEA (Bagnall et al., 2018)
	AtrialFibrillation	0.008 Seconds	38400	UEA (Bagnall et al., 2018)
	PigArtPressure	-	624000	UCR (Dau et al., 2019)
	PIGCVP	-	624000	UCR (Dau et al., 2019)
	TDBrain	0.002 Seconds	79232703	(Wang et al., 2024)
Transport	Pems03	5 Minute	9382464	(Liu et al., 2022)
	Pems07	5 Minute	24921792	(Liu et al., 2022)
	Pems-bay	5 Minute	16937700	(Liu et al., 2022)
	Pedestrian_Counts	Hourly	3132346	Monash (Godahehwa et al., 2021b)
Web	Web Traffic	Daily	116485589	Monash (Godahehwa et al., 2021b)
	Phoneme	-	2160640	UCR(Dau et al., 2019)
	EigenWorms	-	27947136	UEA (Bagnall et al., 2018)
Nature	PRSA	Hourly	4628448	(Zhang et al., 2017)
	Temperature Rain	Daily	23252200	Monash (Godahehwa et al., 2021b)
	StarLightCurves	-	9457664	UCR (Dau et al., 2019)
	Worms	0.033 Seconds	232200	UCR (Dau et al., 2019)
	Saugen River Flow	Daily	23741	Monash (Godahehwa et al., 2021b)
	Sunspot	Daily	73924	Monash (Godahehwa et al., 2021b)
	Weather	Daily	43032000	Monash (Godahehwa et al., 2021b)
	KDD Cup 2018	Daily	2942364	Monash(Godahehwa et al., 2021b)
	US Births	Daily	7305	Monash (Godahehwa et al., 2021b)

A.2. Baselines

For zero-shot deterministic forecasting, we compare the FLAME family against 8 advanced foundation models:

Sundial (Liu et al., 2025d), ROSE (Wang et al., 2025c), Timer (Liu et al., 2024c), MOIRAI (Woo et al., 2024), Chronos (Ansari et al.), LightGTS (Wang et al., 2025b), Time-MoE (Shi et al., 2024), and TinyTTM (Ekambaram et al., 2024). For zero-shot probabilistic forecasting, we compare the FLAME family with 4 foundation models: Sundial (Liu et al., 2025d), MOIRAI (Woo et al., 2024), Chronos (Ansari et al.), and Lag-Llama (Rasul et al., 2023), and 4 advanced end-to-end supervised models including TS-Diff (Kolloviev et al., 2023), TimeGrad (Rasul et al., 2021a), CSDI (Tashiro et al., 2021), and GRU NVP (Rasul et al., 2021b). The corresponding codebases and implementation details are summarized in Table 6.

Table 6. Code repositories for baselines.

Model Types	Models	Code Repositories
End2End	TSDiff	https://github.com/amazon-science/unconditional-time-series-diffusion
	CSDI	https://github.com/ermongroup/CSDI
	TimeGrad	https://github.com/Zjh152/TimeGrad
	GRU NVP	https://github.com/microsoft/ProbTS
Foundation	Sundial	https://github.com/thuml/Sundial
	ROSE	https://github.com/decisionintelligence/TSFM-Bench
	Timer	https://github.com/thuml/Large-Time-Series-Model
	MOIRAI	https://github.com/redoules/moirai
	Chronos	https://github.com/amazon-science/chronos-forecasting
	LightGTS	https://github.com/decisionintelligence/LightGTS
	Time-MoE	https://github.com/Time-MoE/Time-MoE
	Lag-Llama	https://github.com/time-series-foundation-models/lag-llama
	TinyTTM	https://huggingface.co/ibm-granite/granite-timeseries-ttm-r1

A.3. Benchmarks

To thoroughly assess the effectiveness of FLAME, we conduct experiments on TSFM-Bench (Li et al., 2025c) and ProbTS (Zhang et al., 2024). Our evaluation spans 11 deterministic and 9 probabilistic forecasting datasets.

For deterministic forecasting, we use ETTm1, ETTm2, ETTh1, ETTh2, Weather, Electricity, Traffic, Solar, PEMS08, Wind, and NYSE from TSFM-Bench. For most datasets, the prediction length is set to $L \in \{96, 192, 336, 720\}$, while NYSE uses $L \in \{24, 36, 48, 60\}$.

For probabilistic forecasting, we adopt ETTm1, ETTm2, ETTh1, ETTh2, Weather, Electricity, Traffic, Exchange, and ILI from ProbTS. The prediction length is set to $L \in \{96, 192, 336, 720\}$ for most datasets, while ILI-L uses $L \in \{24, 36, 48, 60\}$.

All models are configured with the contextual length of the best performance recommended in their papers. It is important to clarify that datasets shared in both the TSFM-Bench and ProbTS (e.g., ETTh1, Traffic) are different in evaluation settings like strides. A summary of dataset statistics can be found in Table 7.

Table 7. Statistics of benchmark datasets.

Dataset	Domain	Frequency	Lengths	Dim	Split	Stride	Benchmark	Description
ETTm1	Electricity	15 mins	57,600	7	6:2:2	1	TFSM-Bench	Power transformer 1, comprising seven indicators such as oil temperature and useful load
ETTm2	Electricity	15 mins	57,600	7	6:2:2	1	TFSM-Bench	Power transformer 2, comprising seven indicators such as oil temperature and useful load
ETTh1	Electricity	1 hour	14,400	7	6:2:2	1	TFSM-Bench	Power transformer 1, comprising seven indicators such as oil temperature and useful load
ETTh2	Electricity	1 hour	14,400	7	6:2:2	1	TFSM-Bench	Power transformer 2, comprising seven indicators such as oil temperature and useful load
Weather	Environment	10 mins	52,696	21	7:1:2	1	TFSM-Bench	Recorded every for the whole year 2020, which contains 21 meteorological indicators
Electricity	Electricity	1 hour	26,304	321	7:1:2	1	TFSM-Bench	Electricity records the electricity consumption in kWh every 1 hour from 2012 to 2014
Traffic	Traffic	1 hour	17,544	862	7:1:2	1	TFSM-Bench	Road occupancy rates measured by 862 sensors on San Francisco Bay area freeways
Solar	Energy	10 mins	52,560	137	6:2:2	1	TFSM-Bench	Solar production records collected from 137 PV plants in Alabama
PEMS08	Traffic	5 mins	17,856	170	6:2:2	1	TFSM-Bench	Traffic flow time series collected from the CalTrans PeMS
Wind	Energy	15 mins	48,673	7	7:1:2	1	TFSM-Bench	Wind power records from 2020-2021 at 15-minute intervals
NYSE	Stock	1 day	1,243	5	7:1:2	1	TFSM-Bench	Records opening price, closing price, trading volume, lowest price, and highest price
ETTm1	Electricity	15 mins	57,600	7	6:2:2	96	ProbTS	Power transformer 1, comprising seven indicators such as oil temperature and useful load
ETTm2	Electricity	15 mins	57,600	7	6:2:2	96	ProbTS	Power transformer 2, comprising seven indicators such as oil temperature and useful load
ETTh1	Electricity	1 hour	14,400	7	6:2:2	96	ProbTS	Power transformer 1, comprising seven indicators such as oil temperature and useful load
ETTh2	Electricity	1 hour	14,400	7	6:2:2	96	ProbTS	Power transformer 2, comprising seven indicators such as oil temperature and useful load
Weather	Environment	10 mins	52,696	21	7:1:2	96	ProbTS	Recorded every for the whole year 2020, which contains 21 meteorological indicators
Electricity	Electricity	1 hour	26,304	321	7:1:2	96	ProbTS	Electricity records the electricity consumption in kWh every 1 hour from 2012 to 2014
Traffic	Traffic	1 hour	17,544	862	7:1:2	96	ProbTS	Road occupancy rates measured by 862 sensors on San Francisco Bay area freeways
Exchange	Economic	1 day	7,588	8	7:1:2	96	ProbTS	ExchangeRate collects the daily exchange rates of eight countries
ILI	Health	1 week	966	7	7:1:2	96	ProbTS	Recorded indicators of patients data from Centers for Disease Control and Prevention

A.4. Experimental Settings

Pretraining We implement the FLAME family using Distributed Data Parallel in PyTorch (Paszke et al., 2019), and conduct all experiments on 8 NVIDIA A800 GPUs with 80GB GPU memory. The model is optimized using the AdamW optimizer with an initial learning rate of 5×10^{-5} . To progressively reduce the learning rate during training, we employ a step decay schedule via the StepLR scheduler. During pre-training, we use 12 historical tokens and 4 prediction tokens, with a reference patch size $p = 48$. The batch size is set to 8,192. Full details on model configurations and parameter sizes are summarized in Table 8.

Table 8. Detailed model configurations of the FLAME family and corresponding parameter counts.

Models	Encoder Layers	Decoder Layers	Couple Layers	Model Dim d	FFN Dim d'	Parameters
FLAME Small	1	1	3	256	512	2M
FLAME Base	1	3	5	256	512	6M
FLAME Large	1	6	7	256	512	10M

Downstream Forecasting For downstream forecasting tasks, we apply periodic patching strategies adapted to each dataset’s temporal characteristics. The number of past tokens remains fixed at 11, while the prediction lengths are evaluated at 96, 192, 336, and 720 steps.

We also address the “Drop Last” issue highlighted in recent studies (Qiu et al., 2024; 2025c; Li et al., 2025c), where setting `drop_last=True` during test evaluation may lead to misleading results due to incomplete batches. To ensure consistency and fairness, we set `drop_last=False` for all baseline models in our experiments.

A.5. Evaluation Metrics

Regarding evaluation metrics, following the experimental setup in TFSM-Bench, we adopt Mean Squared Error (MSE)

and Mean Absolute Error (MAE) as evaluation metrics for deterministic forecasting. For probabilistic forecasting, we use Continuous Ranked Probability Score (CRPS) and Normalized Mean Absolute Error (NMAE) in ProbTS. Considering the case with K variates and T forecasting horizon.

Mean Squared Error (MSE) The Mean Squared Error quantifies the average of the squared differences between predicted values and their corresponding ground truths. It penalizes larger errors more heavily due to the squaring operation, making it sensitive to outliers. Formally, it is defined as:

$$\text{MSE} = \frac{1}{K \times T} \sum_{k=1}^K \sum_{t=1}^T (x_t^k - \hat{x}_t^k)^2, \quad (33)$$

where K denotes the number of variables, T the prediction horizon, x_t^k the true value, and \hat{x}_t^k the predicted value.

Mean Absolute Error (MAE) The Mean Absolute Error calculates the average magnitude of prediction errors without considering their direction. By focusing on the absolute differences, MAE provides a robust and interpretable measure of accuracy:

$$\text{MAE} = \frac{1}{K \times T} \sum_{k=1}^K \sum_{t=1}^T |x_t^k - \hat{x}_t^k|, \quad (34)$$

where all terms follow the same definition as above. Unlike MSE, MAE treats all errors equally and is less sensitive to large deviations.

Continuous Ranked Probability Score (CRPS) The CRPS assesses the quality of probabilistic forecasts by comparing the predicted cumulative distribution function (CDF) F with the observed outcome x . It is computed as:

$$\text{CRPS} = \int_{\mathbb{R}} (F(z) - \mathbb{I}\{x \leq z\})^2 dz, \quad (35)$$

where $\mathbb{I}\{x \leq z\}$ is the indicator function. CRPS rewards distributions that assign high probability to the true value and achieves its minimum when the predicted distribution matches the true distribution. In practice, we approximate CRPS using the empirical CDF $\hat{F}(z) = \frac{1}{n} \sum_{i=1}^n \mathbb{I}\{X_i \leq z\}$ based on $n = 100$ samples drawn from the conditional predictive distribution $p_{\theta}(x_t | h_t)$.

Normalized Mean Absolute Error (NMAE) The NMAE extends MAE by normalizing it against the total magnitude of ground-truth values, thereby enabling fair comparison across datasets with varying scales. Its formula is:

$$\text{NMAE} = \frac{\sum_{k=1}^K \sum_{t=1}^T |x_t^k - \hat{x}_t^k|}{\sum_{k=1}^K \sum_{t=1}^T |x_t^k|} \quad (36)$$

B. Full Model Analytics

B.1. Analytics of Sampling Number

Given that FLAME models distributions across the forecasting horizon, we conduct an in-depth study on the scalability of generative forecasting by examining the correlations between the sampling number and performance, as presented in Table 9. Specifically, we choose four sampling numbers: 10, 20, 50, and 100. The findings indicate that both CRPS and NMAE demonstrate a consistent improvement as the sampling number rises. Moreover, a sampling number of 100 leads to excellent performance, and this is unlikely to impose significant efficiency burdens in practical applications.

B.2. Analytics of Local-Perception

As shown in Table 10, we select three variants to assess the Local-Perception. These variants include eliminating the entire Local-Perception (termed as “w/o Local-Perception”), encoding the closest single period without performing alignment (referred to as “w/o Period Alignment”), and making the initialized matrices A, B learnable (denoted as “Learnable LegT”). Our observations indicate that Local-Perception indeed has a significant impact. Specifically, the variant lacking Local-Perception experiences a collapse in zero-shot performance. Period Alignment is also of importance. When considering datasets such as Electricity and Traffic, which contain complex periodic information, the zero-shot performance deteriorates substantially without the assistance of Period Alignment. Regarding Learnable LegT, its performance shows a slight decline when the initialized

Table 9. Full results of probabilistic forecasting experiments with different sampling numbers.

Models	FLAME-10		FLAME-20		FLAME-50		FLAME-100		
	Metric	CRPS	NMAE	CRPS	NMAE	CRPS	NMAE	CRPS	NMAE
ETIm1	96	1.255	<u>0.412</u>	0.388	0.477	<u>0.323</u>	0.418	0.315	0.407
	192	0.905	0.444	0.372	0.433	<u>0.358</u>	<u>0.432</u>	0.337	0.426
	336	0.369	0.468	0.448	0.682	<u>0.352</u>	<u>0.448</u>	0.351	0.447
	720	<u>0.388</u>	<u>0.486</u>	0.394	0.491	0.394	0.488	0.383	0.476
	avg	0.729	0.453	0.401	0.521	<u>0.357</u>	<u>0.447</u>	0.347	0.439
ETIm2	96	0.134	0.173	0.129	0.167	<u>0.125</u>	<u>0.163</u>	0.124	0.155
	192	0.208	0.196	0.187	0.190	<u>0.144</u>	<u>0.186</u>	0.143	0.175
	336	0.477	0.212	0.427	0.208	<u>0.159</u>	<u>0.204</u>	0.158	0.193
	720	0.662	0.236	0.631	0.232	<u>0.187</u>	<u>0.229</u>	0.184	0.219
	avg	0.370	0.204	0.344	0.199	<u>0.154</u>	<u>0.196</u>	0.152	0.186
ETTh1	96	0.299	0.346	0.269	0.331	<u>0.262</u>	<u>0.324</u>	0.259	0.310
	192	0.294	0.365	0.285	0.354	<u>0.279</u>	<u>0.347</u>	0.278	0.342
	336	0.309	0.383	0.298	0.372	<u>0.293</u>	<u>0.365</u>	0.290	0.362
	720	0.328	0.406	0.317	0.396	<u>0.311</u>	<u>0.390</u>	0.303	0.367
	avg	0.308	0.375	0.292	0.363	<u>0.286</u>	<u>0.357</u>	0.283	0.345
ETTh2	96	0.158	0.200	0.150	0.191	<u>0.146</u>	<u>0.188</u>	0.144	0.186
	192	0.167	0.211	0.162	0.207	<u>0.160</u>	<u>0.206</u>	0.159	0.204
	336	0.181	0.226	0.176	0.222	<u>0.174</u>	<u>0.221</u>	0.172	0.217
	720	0.191	0.234	0.187	0.231	<u>0.183</u>	<u>0.229</u>	0.182	0.228
	avg	0.174	0.218	0.169	0.213	<u>0.166</u>	<u>0.211</u>	0.164	0.209
Weather	96	0.080	0.098	0.178	0.093	<u>0.073</u>	<u>0.091</u>	0.067	0.083
	192	0.103	0.112	0.092	0.105	<u>0.084</u>	<u>0.103</u>	0.068	0.082
	336	1.382	0.121	0.233	0.117	<u>0.092</u>	<u>0.114</u>	0.079	0.094
	720	2.471	0.133	1.384	0.129	<u>0.101</u>	<u>0.127</u>	0.083	0.100
	avg	1.009	0.116	0.472	0.111	<u>0.088</u>	<u>0.109</u>	0.074	0.090
Electricity	96	1.734	0.097	0.072	0.092	<u>0.070</u>	<u>0.090</u>	0.069	0.089
	192	0.093	0.119	1.662	0.116	<u>0.086</u>	<u>0.112</u>	0.072	0.088
	336	0.662	0.147	0.375	0.143	<u>0.107</u>	<u>0.140</u>	0.081	0.096
	720	2.406	0.173	1.354	0.168	<u>0.125</u>	<u>0.166</u>	0.100	0.116
	avg	1.224	0.134	0.866	0.130	<u>0.097</u>	<u>0.127</u>	0.081	0.097
Traffic	96	0.562	0.301	0.491	0.309	<u>0.224</u>	<u>0.273</u>	0.220	0.268
	192	0.811	0.324	0.681	0.333	<u>0.240</u>	<u>0.298</u>	0.238	0.294
	336	2.911	0.348	3.284	0.364	<u>0.257</u>	<u>0.323</u>	0.254	0.319
	720	3.491	0.378	2.824	0.484	<u>0.278</u>	<u>0.354</u>	0.276	0.351
	avg	1.944	0.338	1.820	0.373	<u>0.250</u>	<u>0.312</u>	0.247	0.308
Exchange	96	0.023	0.027	0.022	0.027	<u>0.022</u>	<u>0.027</u>	0.020	0.026
	192	0.032	0.037	0.032	0.037	<u>0.031</u>	<u>0.037</u>	0.031	0.035
	336	0.045	0.049	0.044	0.049	<u>0.044</u>	<u>0.049</u>	0.044	0.046
	720	1.234	0.098	0.145	0.082	<u>0.074</u>	<u>0.079</u>	0.073	0.079
	avg	0.334	0.053	0.061	0.049	<u>0.043</u>	<u>0.048</u>	0.042	0.047
ILI	24	<u>0.156</u>	<u>0.188</u>	0.157	0.197	0.157	0.194	0.136	0.168
	36	0.178	0.216	0.181	0.225	<u>0.177</u>	<u>0.214</u>	0.145	0.179
	48	0.197	<u>0.234</u>	0.201	0.244	<u>0.196</u>	0.235	0.164	0.200
	60	0.196	0.234	<u>0.190</u>	<u>0.231</u>	0.192	0.233	0.169	0.204
	avg	0.182	<u>0.218</u>	0.182	0.224	<u>0.181</u>	0.219	0.154	0.188

matrices A, B are made learnable. This is because, upon being pretrained on a large-scale time series corpus, the Legendre coefficients within the matrices may gradually change, thereby losing the on-line approximation capability.

Table 10. Experimental results on Local Perception analysis, comparing configurations without Local Perception (LP), without Period Alignment (P.A.), and with Learnable LegT (L.L.).

Models Metric	w/o LP		w/o P.A.		with L.L.		FLAME Large		
	MSE	CRPS	MSE	CRPS	MSE	CRPS	MSE	CRPS	
ETTm1	96	0.365	0.352	0.362	0.332	0.297	0.317	0.301	0.315
	192	0.389	0.385	0.387	0.364	0.327	0.335	0.328	0.337
	336	0.417	0.407	0.408	0.398	0.353	0.359	0.351	0.351
	720	0.470	0.462	0.483	0.423	0.397	0.390	0.392	0.383
	avg	0.410	0.402	0.410	0.379	0.344	0.350	0.343	0.347
ETTm2	96	0.229	0.144	0.216	0.133	0.178	0.121	0.186	0.124
	192	0.283	0.154	0.258	0.149	0.253	0.146	0.247	0.143
	336	0.311	0.186	0.304	0.171	0.297	0.164	0.300	0.158
	720	0.362	0.200	0.363	0.195	0.365	0.191	0.357	0.184
	avg	0.296	0.171	0.285	0.162	0.273	0.156	0.273	0.152
ETTTh1	96	0.372	0.283	0.362	0.279	0.352	0.255	0.358	0.259
	192	0.418	0.304	0.402	0.291	0.408	0.291	0.392	0.278
	336	0.433	0.322	0.428	0.300	0.413	0.304	0.411	0.290
	720	0.450	0.376	0.459	0.318	0.438	0.328	0.444	0.303
	avg	0.418	0.321	0.413	0.297	0.403	0.295	0.401	0.283
ETTTh2	96	0.312	0.148	0.303	0.145	0.311	0.161	0.300	0.144
	192	0.368	0.167	0.358	0.159	0.364	0.178	0.351	0.159
	336	0.384	0.182	0.375	0.174	0.391	0.199	0.374	0.172
	720	0.425	0.188	0.422	0.186	0.422	0.185	0.416	0.182
	avg	0.372	0.171	0.365	0.166	0.372	0.181	0.360	0.164
Weather	96	0.233	0.076	0.195	0.071	0.168	0.067	0.152	0.067
	192	0.270	0.099	0.225	0.074	0.214	0.069	0.199	0.068
	336	0.295	0.112	0.261	0.088	0.255	0.078	0.250	0.079
	720	0.312	0.127	0.311	0.098	0.312	0.081	0.307	0.083
	avg	0.278	0.104	0.248	0.083	0.237	0.074	0.227	0.074
Electricity	96	0.214	0.088	0.202	0.077	0.166	0.072	0.161	0.069
	192	0.253	0.098	0.237	0.091	0.198	0.073	0.190	0.072
	336	0.309	0.112	0.288	0.104	0.233	0.085	0.227	0.081
	720	0.397	0.138	0.374	0.112	0.292	0.105	0.289	0.100
	avg	0.293	0.109	0.275	0.096	0.222	0.084	0.217	0.081
Traffic	96	0.599	0.239	0.557	0.229	0.503	0.222	0.480	0.220
	192	0.631	0.275	0.592	0.251	0.526	0.246	0.511	0.238
	336	0.722	0.301	0.647	0.282	0.589	0.265	0.553	0.254
	720	0.808	0.318	0.712	0.294	0.647	0.279	0.639	0.276
	avg	0.690	0.283	0.627	0.264	0.566	0.253	0.546	0.247

B.3. Analytics of SSD-Decoder

Subsequently, we conduct a comparison between the SSD-Decoder and the decoders of other mechanisms in Table 11. More precisely, we select the Self-Attention Decoder, Causal-Attention Decoder, and Mamba v1 Decoder as the baselines. In the context of forecasting tasks, causal correlations are more suitable. As a result, the Self-Attention Decoder exhibits the poorest performance. We further note that the SSD-Decoder outperforms both the Mamba v1 Decoder and the Causal-Attention Decoder, which showcases its superior ability to leverage memory during the forecasting process.

Table 11. Forecasting performance comparison of different decoders: Self-Attention (SA), Causal-Attention (CA), Mamba v1, and our SSD-Decoder used in FLAME.

Models Metric	SA		CA		Mamba v1		FLAME		
	MSE	CRPS	MSE	CRPS	MSE	CRPS	MSE	CRPS	
ETTm1	96	0.389	0.448	0.377	0.358	0.337	0.332	0.301	0.315
	192	0.421	0.467	0.395	0.382	0.359	0.341	0.328	0.337
	336	0.449	0.485	0.413	0.401	0.390	0.367	0.351	0.351
	720	0.491	0.508	0.461	0.442	0.444	0.390	0.392	0.383
	avg	0.438	0.477	0.412	0.396	0.383	0.358	0.343	0.347
ETTm2	96	0.235	0.167	0.209	0.141	0.212	0.139	0.186	0.124
	192	0.272	0.198	0.251	0.167	0.256	0.162	0.247	0.143
	336	0.352	0.223	0.313	0.182	0.292	0.179	0.300	0.158
	720	0.398	0.257	0.368	0.224	0.356	0.198	0.357	0.184
	avg	0.314	0.211	0.285	0.179	0.279	0.170	0.273	0.152
ETTTh1	96	0.358	0.269	0.354	0.263	0.363	0.271	0.358	0.259
	192	0.404	0.302	0.395	0.286	0.404	0.303	0.392	0.278
	336	0.420	0.331	0.423	0.297	0.428	0.325	0.411	0.290
	720	0.455	0.352	0.475	0.325	0.468	0.344	0.444	0.303
	avg	0.409	0.314	0.412	0.293	0.416	0.311	0.401	0.283
ETTTh2	96	0.336	0.175	0.288	0.139	0.303	0.148	0.300	0.144
	192	0.382	0.203	0.362	0.170	0.370	0.172	0.351	0.159
	336	0.414	0.212	0.389	0.177	0.401	0.186	0.374	0.172
	720	0.472	0.209	0.432	0.198	0.409	0.202	0.416	0.182
	avg	0.401	0.200	0.368	0.171	0.371	0.177	0.360	0.164
Weather	96	0.188	0.088	0.209	0.093	0.207	0.087	0.152	0.067
	192	0.221	0.094	0.237	0.097	0.237	0.091	0.199	0.068
	336	0.275	0.113	0.261	0.105	0.269	0.102	0.250	0.079
	720	0.328	0.127	0.311	0.117	0.311	0.112	0.307	0.083
	avg	0.253	0.106	0.255	0.103	0.256	0.098	0.227	0.074
Electricity	96	0.210	0.115	0.172	0.075	0.163	0.072	0.161	0.069
	192	0.255	0.127	0.204	0.084	0.191	0.077	0.190	0.072
	336	0.318	0.132	0.243	0.098	0.234	0.090	0.227	0.081
	720	0.415	0.149	0.302	0.122	0.285	0.108	0.289	0.100
	avg	0.300	0.131	0.230	0.095	0.218	0.087	0.217	0.081
Traffic	96	0.587	0.311	0.492	0.238	0.501	0.244	0.480	0.220
	192	0.617	0.338	0.521	0.256	0.522	0.270	0.511	0.238
	336	0.662	0.343	0.572	0.275	0.562	0.294	0.553	0.254
	720	0.749	0.372	0.655	0.294	0.642	0.298	0.639	0.276
	avg	0.654	0.341	0.560	0.266	0.557	0.277	0.546	0.247

B.4. Analytics of Flow-based Head

To assess the efficacy of the Flow-based Head, we choose alternative generative mechanisms to implement forecasting heads as baselines—see Table 12. These include Variational AutoEncoder (VAE), Diffusion, and Flow Match. Given that the VAE adheres to a one-step generation paradigm, it exhibits subpar performance in scenarios such as Electricity

and Traffic. This is because accurately generating distributions over the complex real-world forecasting horizon in these scenarios poses a significant challenge. Regarding Diffusion and Flow Match, although they possess robust multi-step generation paradigms, our findings indicate that they are not as potent as our meticulously-designed Flow-based Head.

Table 12. Forecasting performance comparison of various generative heads: VAE, Diffusion, Flow Match, and our Flow-based Head used in FLAME.

Models	VAE		Diffusion		Flow Match		FLAME		
	MSE	CRPS	MSE	CRPS	MSE	CRPS	MSE	CRPS	
ETTh1	96	0.334	0.348	<u>0.305</u>	<u>0.318</u>	0.311	0.323	0.301	0.315
	192	0.364	0.382	0.340	0.345	<u>0.331</u>	<u>0.340</u>	0.328	0.337
	336	0.388	0.397	<u>0.359</u>	0.362	0.361	<u>0.360</u>	0.351	0.351
	720	0.421	0.448	0.401	0.390	<u>0.398</u>	<u>0.386</u>	0.392	0.383
	avg	0.377	0.394	0.351	0.354	<u>0.350</u>	<u>0.352</u>	0.343	0.347
ETTh2	96	0.223	0.152	<u>0.194</u>	<u>0.128</u>	0.215	0.139	0.186	0.124
	192	0.292	0.179	0.261	0.145	<u>0.257</u>	<u>0.144</u>	0.247	0.143
	336	0.345	0.197	0.322	<u>0.163</u>	<u>0.309</u>	0.168	0.300	0.158
	720	0.392	0.215	<u>0.370</u>	<u>0.200</u>	0.381	0.205	0.357	0.184
	avg	0.313	0.186	<u>0.287</u>	<u>0.159</u>	0.291	0.164	0.273	0.152
ETTh1	96	0.366	0.279	<u>0.359</u>	<u>0.261</u>	0.363	0.267	0.358	0.259
	192	0.398	<u>0.285</u>	<u>0.394</u>	0.288	0.404	0.295	0.392	0.278
	336	<u>0.423</u>	<u>0.301</u>	0.428	0.318	0.427	0.330	0.411	0.290
	720	<u>0.457</u>	<u>0.320</u>	0.479	0.348	0.462	0.327	0.444	0.303
	avg	<u>0.411</u>	<u>0.296</u>	0.415	0.304	0.414	0.305	0.401	0.283
ETTh2	96	0.296	0.142	0.332	0.169	0.328	0.164	<u>0.300</u>	<u>0.144</u>
	192	0.358	<u>0.167</u>	0.378	0.180	0.364	0.168	0.351	0.159
	336	0.379	<u>0.182</u>	0.394	0.198	0.384	0.191	0.374	0.172
	720	0.425	<u>0.197</u>	0.448	0.215	0.428	0.202	0.416	0.182
	avg	<u>0.365</u>	<u>0.172</u>	0.388	0.191	0.376	0.181	0.360	0.164
Weather	96	0.176	0.083	0.149	<u>0.068</u>	0.155	0.072	<u>0.152</u>	0.067
	192	0.229	0.086	<u>0.199</u>	<u>0.069</u>	0.206	0.074	0.199	0.068
	336	0.292	0.098	<u>0.256</u>	<u>0.083</u>	0.257	0.084	0.250	0.079
	720	0.357	0.105	0.314	0.089	<u>0.312</u>	<u>0.088</u>	0.307	0.083
	avg	0.264	0.093	<u>0.230</u>	<u>0.077</u>	0.233	0.080	0.227	0.074
Electricity	96	0.241	0.129	0.172	0.078	<u>0.167</u>	<u>0.075</u>	0.161	0.069
	192	0.260	0.134	0.199	0.079	<u>0.195</u>	<u>0.079</u>	0.190	0.072
	336	0.304	0.142	0.251	0.088	<u>0.246</u>	<u>0.086</u>	0.227	0.081
	720	0.357	0.147	0.318	<u>0.105</u>	<u>0.318</u>	0.110	0.289	0.100
	avg	0.291	0.138	0.235	0.088	<u>0.232</u>	<u>0.088</u>	0.217	0.081
Traffic	96	0.721	0.482	<u>0.488</u>	<u>0.236</u>	0.507	0.248	0.480	0.220
	192	0.742	0.498	<u>0.528</u>	<u>0.264</u>	0.557	0.296	0.511	0.238
	336	0.747	0.512	<u>0.572</u>	<u>0.270</u>	0.603	0.305	0.553	0.254
	720	0.769	0.532	<u>0.682</u>	<u>0.293</u>	0.712	0.337	0.639	0.276
	avg	0.745	0.506	<u>0.568</u>	<u>0.266</u>	0.595	0.297	0.546	0.247

C. Full Results

C.1. Full zero-shot results

We provide all the results of the zero-shot deterministic forecasting in Table 13. As shown in Table 13, we include 11 representative real-world datasets from TSFM-Bench, demonstrating that FLAME achieves state-of-the-art forecasting performance.

We provide all the results of the zero-shot probabilistic forecasting in Table 14. As shown in Table 14, we include 9 representative real-world datasets from ProbTS, demonstrating that FLAME achieves state-of-the-art forecasting

performance.

Considering short-term forecasting, we also conduct experiments on 8,068 univariate datasets in TFB (Qiu et al., 2024), we report the average MASE and msMAPE results in Figures 6 and 7. FLAME Large outperforms all baselines including end-to-end supervised models and foundation models.

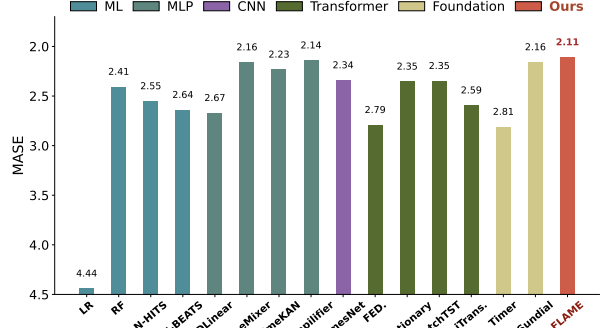


Figure 6. The average MASE results of 8068 datasets in TFB.

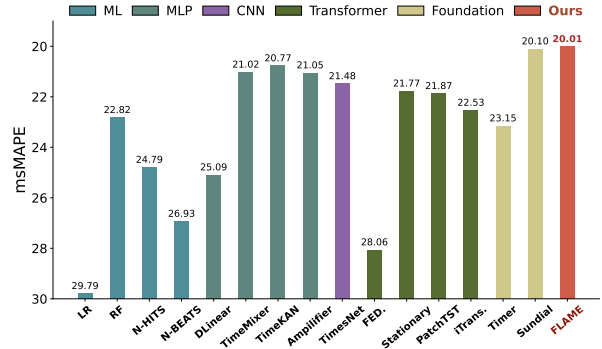


Figure 7. The average msMAPE results of 8068 datasets in TFB.

C.2. Full-shot and few-shot results

We further compare FLAME Small with end-to-end supervised models. We provide all the results of deterministic forecasting in Table 15, comparing FLAME Small of different training budgets with most advanced end-to-end deterministic forecasting models.

We also provide all the results of probabilistic forecasting in Table 16, comparing FLAME Small of different training budgets with most advanced end-to-end probabilistic forecasting models.

D. Showcases

We visualized the forecasting results of FLAME Large on TSFM-Bench and TFB in Figures 8 and 9.

FLAME: Flow Enhanced Legendre Memory Models for General Time Series Forecasting

Table 13. Full results of zero-shot deterministic forecasting experiments on datasets from TSFM-Bench. Lower MSE or MAE values indicate better predictions. ('-') denotes datasets included in the model’s pretraining and therefore excluded from testing. **Red**: the best, **Blue**: the 2nd best.

Models	FLAME Small		FLAME Base		FLAME Large		Sundial (2025)		LightGTS (2025)		ROSE (2025)		Timer (2024)		Chronos (2024)		Time-MoE (2024)		TinyTTM (2024)		MOIRAI (2024)		
	MSE	MAE	MSE	MAE	MSE	MAE	MSE	MAE	MSE	MAE	MSE	MAE	MSE	MAE	MSE	MAE	MSE	MAE	MSE	MAE	MSE	MAE	
ETTm1	96	0.305	0.353	0.298	0.351	0.301	0.353	0.280	0.334	0.307	0.359	0.512	0.460	0.817	0.611	0.402	0.373	0.281	0.341	0.738	0.541	0.353	0.363
	192	0.328	0.370	0.324	0.369	0.328	0.373	0.321	0.366	0.332	0.374	0.512	0.462	0.927	0.659	0.510	0.435	0.305	0.358	0.698	0.547	0.376	0.380
	336	0.349	0.384	0.346	0.386	0.351	0.389	0.350	0.389	0.353	0.393	0.523	0.470	1.043	0.704	0.590	0.477	0.369	0.395	0.670	0.533	0.399	0.395
	720	0.392	0.416	0.385	0.414	0.392	0.419	0.394	0.418	0.388	0.386	0.552	0.490	1.044	0.722	0.703	0.525	0.469	0.472	0.660	0.550	0.432	0.417
	Avg	0.344	0.381	0.338	0.380	0.343	0.384	0.336	0.377	0.345	0.378	0.525	0.471	0.958	0.674	0.551	0.453	0.356	0.392	0.692	0.543	0.390	0.389
ETTm2	96	0.165	0.255	0.171	0.262	0.186	0.272	0.170	0.256	0.166	0.260	0.224	0.309	0.225	0.300	0.192	0.263	0.198	0.288	0.226	0.309	0.189	0.260
	192	0.217	0.297	0.227	0.302	0.247	0.315	0.229	0.300	0.222	0.300	0.266	0.333	0.286	0.339	0.256	0.308	0.235	0.312	0.311	0.360	0.247	0.300
	336	0.262	0.330	0.280	0.340	0.300	0.352	0.281	0.337	0.267	0.333	0.310	0.358	0.335	0.369	0.315	0.346	0.293	0.348	0.350	0.383	0.295	0.334
	720	0.333	0.379	0.348	0.387	0.357	0.394	0.351	0.387	0.340	0.378	0.399	0.407	0.414	0.416	0.409	0.405	0.427	0.428	0.446	0.435	0.372	0.386
	Avg	0.244	0.315	0.257	0.323	0.273	0.333	0.258	0.320	0.249	0.318	0.299	0.352	0.315	0.356	0.293	0.331	0.288	0.344	0.333	0.372	0.276	0.320
ETTl1	96	0.362	0.395	0.361	0.392	0.358	0.389	0.348	0.385	0.359	0.390	0.382	0.408	0.454	0.434	0.444	0.409	0.349	0.379	0.364	0.389	0.380	0.398
	192	0.406	0.427	0.400	0.422	0.392	0.416	0.393	0.418	0.390	0.409	0.400	0.420	0.522	0.465	0.502	0.443	0.395	0.413	0.386	0.407	0.440	0.434
	336	0.436	0.449	0.417	0.436	0.411	0.432	0.422	0.440	0.420	0.436	0.404	0.426	0.559	0.484	0.580	0.460	0.447	0.453	0.404	0.422	0.514	0.474
	720	0.471	0.482	0.433	0.459	0.444	0.463	0.481	0.493	0.437	0.460	0.420	0.447	0.714	0.549	0.605	0.495	0.457	0.462	0.424	0.448	0.705	0.568
	Avg	0.419	0.438	0.403	0.427	0.401	0.425	0.411	0.434	0.402	0.424	0.402	0.425	0.562	0.483	0.533	0.452	0.412	0.427	0.395	0.417	0.510	0.469
ETTl2	96	0.278	0.339	0.295	0.345	0.300	0.350	0.271	0.333	0.278	0.342	0.298	0.362	0.316	0.359	0.306	0.338	0.292	0.352	0.277	0.335	0.287	0.325
	192	0.336	0.381	0.353	0.388	0.351	0.390	0.327	0.376	0.345	0.383	0.336	0.385	0.374	0.398	0.396	0.394	0.347	0.379	0.334	0.373	0.347	0.367
	336	0.373	0.410	0.373	0.409	0.374	0.411	0.354	0.402	0.394	0.416	0.353	0.399	0.381	0.410	0.423	0.417	0.406	0.419	0.362	0.402	0.377	0.393
	720	0.411	0.441	0.413	0.440	0.416	0.444	0.381	0.435	0.430	0.445	0.395	0.432	0.408	0.434	0.442	0.439	0.439	0.447	0.408	0.444	0.404	0.421
	Avg	0.350	0.393	0.359	0.396	0.360	0.399	0.333	0.387	0.362	0.397	0.346	0.395	0.370	0.400	0.392	0.397	0.371	0.399	0.345	0.389	0.354	0.377
Weather	96	0.148	0.204	0.151	0.209	0.152	0.211	0.157	0.205	0.151	0.211	0.200	0.260	0.190	0.236	0.186	0.208	0.157	0.211	0.183	0.242	0.177	0.208
	192	0.189	0.243	0.194	0.250	0.199	0.254	0.205	0.251	0.191	0.248	0.239	0.288	0.261	0.293	0.238	0.258	0.208	0.256	0.229	0.285	0.219	0.249
	336	0.233	0.278	0.241	0.286	0.250	0.293	0.253	0.289	0.236	0.284	0.279	0.315	0.332	0.340	0.313	0.353	0.255	0.290	0.289	0.330	0.277	0.292
	720	0.289	0.320	0.301	0.330	0.307	0.333	0.320	0.336	0.299	0.323	0.340	0.357	0.385	0.381	0.416	0.415	0.405	0.397	0.359	0.370	0.365	0.350
	Avg	0.215	0.261	0.222	0.269	0.227	0.273	0.234	0.270	0.219	0.267	0.265	0.305	0.292	0.313	0.288	0.309	0.256	0.289	0.265	0.307	0.260	0.275
Electricity	96	0.206	0.294	0.170	0.269	0.161	0.261	0.132	0.229	0.181	0.272	0.209	0.307	0.210	0.312	-	-	-	-	0.166	0.263	0.152	0.242
	192	0.247	0.338	0.198	0.298	0.190	0.292	0.152	0.250	0.195	0.284	0.219	0.315	0.239	0.337	-	-	-	-	0.191	0.286	0.171	0.259
	336	0.310	0.398	0.230	0.331	0.227	0.326	0.173	0.271	0.253	0.338	0.236	0.330	0.284	0.372	-	-	-	-	0.237	0.336	0.192	0.278
	720	0.383	0.455	0.288	0.379	0.289	0.372	0.218	0.311	0.304	0.382	0.273	0.328	0.456	0.479	-	-	-	-	0.292	0.384	0.236	0.313
	Avg	0.287	0.371	0.222	0.319	0.217	0.313	0.169	0.265	0.233	0.319	0.234	0.320	0.297	0.375	-	-	-	-	0.222	0.317	0.188	0.273
Traffic	96	0.591	0.401	0.522	0.360	0.480	0.344	-	-	0.525	0.356	0.572	0.407	0.526	0.368	0.562	0.378	-	-	0.514	0.347	-	-
	192	0.623	0.431	0.538	0.374	0.511	0.369	-	-	0.547	0.365	0.575	0.406	0.561	0.385	0.579	0.412	-	-	0.543	0.373	-	-
	336	0.697	0.485	0.574	0.400	0.553	0.394	-	-	0.645	0.419	0.588	0.411	0.614	0.412	0.594	0.420	-	-	0.575	0.389	-	-
	720	0.782	0.528	0.669	0.449	0.639	0.429	-	-	0.722	0.457	0.618	0.422	0.749	0.464	0.723	0.472	-	-	0.622	0.433	-	-
	Avg	0.673	0.461	0.576	0.396	0.546	0.384	-	-	0.610	0.399	0.588	0.412	0.613	0.407	0.615	0.421	-	-	0.564	0.386	-	-
Solar	96	0.185	0.263	0.167	0.259	0.153	0.255	0.204	0.230	0.209	0.309	0.524	0.557	0.591	0.504	0.373	0.304	0.304	0.345	0.863	0.664	0.682	0.688
	192	0.201	0.276	0.180	0.273	0.165	0.269	0.221	0.248	0.220	0.315	0.507	0.550	0.689	0.567	0.363	0.303	0.309	0.342	0.823	0.695	0.694	0.695
	336	0.212	0.283	0.190	0.282	0.174	0.278	0.225	0.260	0.228	0.314	0.508	0.553	0.831	0.636	0.391	0.319	0.433	0.450	0.835	0.741	0.719	0.706
	720	0.213	0.291	0.198	0.295	0.179	0.287	0.233	0.272	0.218	0.283	0.479	0.534	0.972	0.710	0.444	0.349	0.599	0.576	0.738	0.738	0.759	0.725
	Avg	0.203	0.278	0.184	0.277	0.168	0.272	0.221	0.252	0.219	0.305	0.505	0.549	0.771	0.604	0.393	0.319	0.411	0.428	0.815	0.710	0.714	0.704
PEMS08	96	0.249	0.357	0.241	0.353	0.224	0.331	-	-	0.608	0.562	1.373	0.995	0.625	0.580	1.538	0.983	-	-	1.284	0.888	-	-
	192	0.299	0.375	0.288	0.368	0.273	0.342	-	-	0.774	0.648	1.365	0.979	0.798	0.661	1.719	0.983	-	-	1.638	1.039	-	-
	336	0.330	0.376	0.324	0.367	0.305	0.348	-	-	0.892	0.693	1.338	0.960	0.910	0.716	1.768	0.998	-	-	1.979	1.160	-	-
	720	0.418	0.428	0.395	0.406	0.368	0.384	-	-	0.975	0.864	1.401	0.980	1.131	0.824	1.802	1.133	-	-	2.020	1.175	-	-
	Avg	0.324	0.384	0.312																			

FLAME: Flow Enhanced Legendre Memory Models for General Time Series Forecasting

Table 14. Full results of zero-shot probabilistic forecasting experiments on datasets from ProbTS. Lower CRPS or NMAE values indicate better predictions. ('-') denotes datasets included in the model's pretraining and therefore excluded from testing. ('/') denotes the excessive time consumption. **Red**: the best, **Blue**: the 2nd best.

Models	FLAME Small (Ours)		FLAME Base (Ours)		FLAME Large (Ours)		Sundial (2025)		Chronos (2024)		MOIRAI (2024)		Lag-Llama (2023)		TSDiff (2023)		CSDI (2022)		TimeGrad (2022)		GRU NVP (2021)		
	CRPS	NMAE	CRPS	NMAE	CRPS	NMAE	CRPS	NMAE	CRPS	NMAE	CRPS	NMAE	CRPS	NMAE	CRPS	NMAE	CRPS	NMAE	CRPS	NMAE	CRPS	NMAE	
ETTm1	96	0.294	0.368	0.326	0.417	0.315	0.407	<u>0.253</u>	<u>0.308</u>	0.360	0.422	0.464	0.522	0.354	0.402	0.344	0.441	0.236	0.308	0.522	0.645	0.383	0.488
	192	0.332	0.420	0.363	0.469	0.337	0.426	0.279	0.337	0.404	0.450	0.467	0.531	0.368	0.415	0.345	0.441	<u>0.291</u>	<u>0.377</u>	0.603	0.748	0.396	0.514
	336	0.341	0.427	0.393	0.511	0.351	0.447	0.291	0.350	0.425	0.456	0.524	0.558	0.387	0.436	0.462	0.571	<u>0.322</u>	<u>0.419</u>	0.601	0.759	0.486	0.630
	720	<u>0.364</u>	<u>0.454</u>	0.477	0.622	0.383	0.476	0.318	0.380	0.461	0.478	0.514	0.535	0.403	0.466	0.478	0.622	0.448	0.578	0.621	0.793	0.546	0.707
	avg	0.333	<u>0.417</u>	0.390	0.505	0.347	0.439	0.285	0.344	0.413	0.451	0.492	0.536	0.378	0.430	0.407	0.519	<u>0.324</u>	0.421	0.587	0.736	0.453	0.585
ETTm2	96	<u>0.120</u>	<u>0.153</u>	0.121	0.153	0.124	0.155	0.128	0.153	0.134	0.158	0.176	0.186	0.163	0.192	0.175	0.224	0.115	0.146	0.427	0.525	0.319	0.413
	192	<u>0.146</u>	0.182	0.147	0.184	0.143	0.175	0.150	<u>0.177</u>	0.163	0.183	0.197	0.207	0.181	0.207	0.255	0.316	0.147	0.189	0.424	0.530	0.326	0.427
	336	<u>0.163</u>	0.202	0.164	0.205	0.158	0.193	0.167	<u>0.195</u>	0.190	0.204	0.229	0.227	0.206	0.229	0.328	0.397	0.190	0.248	0.469	0.566	0.449	0.580
	720	<u>0.185</u>	0.223	0.186	0.231	0.184	0.219	0.189	0.217	0.223	0.230	0.321	0.258	0.227	0.249	0.344	0.416	0.239	0.306	0.470	0.561	0.561	0.749
	avg	<u>0.154</u>	0.190	0.155	0.193	0.152	0.186	0.158	<u>0.186</u>	0.178	0.194	0.231	0.220	0.194	0.219	0.276	0.338	0.173	0.222	0.448	0.546	0.414	0.542
ETT1	96	0.265	0.322	<u>0.282</u>	0.319	0.259	<u>0.310</u>	<u>0.260</u>	0.307	0.293	0.341	0.469	0.488	0.297	0.340	0.395	0.510	0.437	0.557	0.455	0.585	0.379	0.481
	192	0.288	<u>0.346</u>	<u>0.281</u>	0.351	0.278	0.342	0.297	<u>0.347</u>	0.348	0.384	0.496	0.492	0.312	0.356	0.496	0.596	0.496	0.625	0.516	0.680	0.425	0.531
	336	0.300	0.371	<u>0.297</u>	0.368	0.290	0.362	0.314	<u>0.365</u>	0.384	0.409	0.503	0.489	0.326	0.370	0.450	0.581	0.454	0.574	0.512	0.666	0.458	0.580
	720	0.320	0.402	<u>0.312</u>	0.386	0.303	<u>0.367</u>	0.312	<u>0.366</u>	0.413	0.425	0.526	0.508	0.340	0.405	0.516	0.657	0.528	0.657	0.523	0.672	0.502	0.643
	avg	0.293	0.360	<u>0.288</u>	0.356	0.283	0.345	0.296	<u>0.346</u>	0.360	0.390	0.498	0.494	0.319	0.368	0.457	0.586	0.479	0.603	0.502	0.651	0.441	0.559
ETT2	96	0.139	0.177	0.145	<u>0.185</u>	<u>0.144</u>	0.186	0.157	0.186	0.163	0.191	0.212	0.238	0.178	0.204	0.336	0.421	0.164	0.214	0.358	0.448	0.432	0.548
	192	0.152	0.195	0.161	0.207	<u>0.159</u>	<u>0.204</u>	0.183	0.213	0.195	0.218	0.229	0.250	0.193	0.217	0.265	0.339	0.226	0.294	0.457	0.575	0.625	0.766
	336	0.170	0.216	0.174	0.224	<u>0.172</u>	<u>0.217</u>	0.203	0.232	0.226	0.241	0.253	0.263	0.211	0.230	0.350	0.427	0.274	0.353	0.481	0.606	0.793	0.942
	720	<u>0.183</u>	<u>0.231</u>	0.191	0.241	0.182	0.228	0.203	0.233	0.255	0.263	0.279	0.273	0.222	0.238	0.406	0.482	0.302	0.382	0.445	0.550	0.539	0.688
	avg	0.161	0.205	0.168	0.214	<u>0.164</u>	<u>0.209</u>	0.186	0.216	0.210	0.228	0.243	0.256	0.201	0.222	0.339	0.417	0.242	0.311	0.435	0.545	0.597	0.736
Weather	96	0.071	0.088	0.071	<u>0.085</u>	0.067	0.083	0.078	0.091	0.136	0.155	0.161	0.141	0.085	0.094	0.104	0.113	<u>0.068</u>	0.087	0.130	0.164	0.116	0.145
	192	0.089	0.113	0.081	0.100	0.068	0.082	0.083	0.097	0.145	0.165	0.173	0.139	0.094	0.102	0.134	0.144	<u>0.068</u>	<u>0.086</u>	0.127	0.158	0.122	0.147
	336	0.094	0.121	0.090	0.110	0.079	0.094	0.090	0.106	0.136	0.151	0.149	0.134	0.098	0.109	0.137	0.138	<u>0.083</u>	<u>0.098</u>	0.130	0.162	0.128	0.160
	720	0.103	0.132	0.106	0.125	0.083	0.100	0.096	0.113	0.151	0.161	0.233	0.155	0.107	0.120	0.152	0.141	<u>0.087</u>	<u>0.102</u>	0.113	0.136	0.110	0.135
	avg	0.089	0.114	0.087	0.105	0.074	0.090	0.087	0.102	0.142	0.158	0.179	0.143	0.096	0.106	0.132	0.134	<u>0.077</u>	<u>0.093</u>	0.125	0.155	0.119	0.147
Electricity	96	0.071	0.090	<u>0.066</u>	<u>0.084</u>	0.069	0.089	<u>0.068</u>	0.083	-	-	0.231	0.275	-	-	0.344	0.441	0.153	0.203	0.096	0.119	0.094	0.118
	192	0.086	0.103	0.076	0.098	0.072	0.088	<u>0.074</u>	<u>0.090</u>	-	-	0.236	0.279	-	-	0.345	0.441	0.200	0.264	0.100	0.124	0.097	0.121
	336	0.096	0.125	0.091	0.117	0.081	0.096	<u>0.083</u>	<u>0.100</u>	-	-	0.245	0.289	-	-	0.462	0.571	/	/	0.102	0.126	0.099	0.123
	720	0.117	0.154	0.110	0.141	<u>0.100</u>	<u>0.116</u>	0.098	<u>0.118</u>	-	-	0.274	0.318	-	-	0.478	0.622	/	/	0.108	0.134	0.114	0.144
	avg	0.093	0.118	0.086	0.110	0.081	0.097	<u>0.081</u>	<u>0.098</u>	-	-	0.247	0.290	-	-	0.407	0.519	/	/	0.102	0.126	0.101	0.127
Traffic	96	0.240	0.293	0.229	0.277	0.220	0.268	-	-	0.250	0.289	-	-	0.255	0.297	0.294	0.342	/	/	<u>0.202</u>	<u>0.234</u>	0.187	0.231
	192	0.257	0.319	0.239	0.291	0.238	0.294	-	-	0.249	0.278	-	-	0.295	0.343	0.306	0.354	/	/	<u>0.208</u>	<u>0.239</u>	0.192	0.236
	336	0.271	0.341	0.250	0.311	0.254	0.319	-	-	0.269	0.290	-	-	0.335	0.384	0.317	0.392	/	/	<u>0.213</u>	<u>0.246</u>	0.201	0.248
	720	0.304	0.395	0.274	0.346	0.276	0.351	-	-	0.310	0.321	-	-	0.434	0.517	0.391	0.478	/	/	<u>0.220</u>	<u>0.263</u>	0.211	<u>0.264</u>
	avg	0.268	0.337	0.248	0.306	0.247	0.308	-	-	0.269	0.295	-	-	0.330	0.385	0.327	0.392	/	/	<u>0.211</u>	<u>0.246</u>	0.198	0.245
Exchange	96	0.023	0.028	<u>0.021</u>	0.027	0.020	<u>0.026</u>	0.024	0.027	0.021	0.025	0.025	0.030	0.042	0.051	0.079	0.090	0.028	0.036	0.068	0.079	0.071	0.091
	192	0.032	0.037	0.030	0.036	<u>0.031</u>	0.035	0.034	0.038	0.032	<u>0.036</u>	0.034	0.039	0.047	0.058	0.093	0.106	0.045	0.058	0.087	0.100	0.068	0.087
	336	<u>0.044</u>	0.049	0.041	<u>0.047</u>	0.044	0.046	0.046	0.050	0.045	0.048	0.047	0.052	0.061	0.073	0.081	0.106	0.060	0.076	0.074	0.086	0.072	0.091
	720	0.074	<u>0.079</u>	0.069	0.077	<u>0.073</u>	0.079	0.076	0.079	0.078	0.080	0.073	0.081	0.078	0.094	0.082	0.142	0.143	0.073	0.099	0.113	0.099	0.103
	avg	0.043	0.048	0.040	<u>0.047</u>	<u>0.042</u>	0.047	0.045	0.049	0.044	0.047	0.045	0.050	0.057	0.069	0.084	0.111	0.069	0.086	0.082	0.095	0.073	0.093
ILI	24	0.135	0.166	<u>0.111</u>	0.143	0.136	0.168	0.108	0.123	0.120	<u>0.139</u>	0.150	0.196	0.135	0.173	0.228	0.242	0.250	0.263	0.275	0.296	0.257	0.283
	36	0.164	0.200	0.119	0.153	<u>0.145</u>	0.179	0.152	<u>0.169</u>	0.179	0.205	0.171	0.222	0.163	0.227	0.235	0.246	0.285	0.298	0.272	0.298	0.281	0.307
	48	0.176	0.216	0.139	0.178	0.164	0.200	0.164	0.184	0.186	0.215	<u>0.151</u>	<u>0.184</u>	0.171	0.233	0.265	0.275	0.285	0.301	0.295	0.320	0.288	0.314
	60	0.171	0.211	0.149	<u>0.189</u>	0.169	0.204	0.168	0.190	0.196	0.228	0.163	0.188	<u>0.156</u>	0.211	0.263	0.272	0.28					

Table 15. Deterministic forecasting results. Full-shot, 10% few-shot and zero-shot results of FLAME Small v.s most advanced end-to-end supervised models on commonly-used datasets in TSFM-Bench. Lower MSE or MAE values indicate better predictions. **Red**: the best, **Blue**: the second best.

Models	FLAME Small (Zero-shot)		FLAME Small (10% few-shot)		FLAME Small (Full-shot)		TimeKAN (2025)		AMD (2025)		TimePro (2025)		TimeXer (2024)		Fredformer (2024)		iTransformer (2024)		PatchTST (2023)		TimesNet (2023)		
	MSE	MAE	MSE	MAE	MSE	MAE	MSE	MAE	MSE	MAE	MSE	MAE	MSE	MAE	MSE	MAE	MSE	MAE	MSE	MAE	MSE	MAE	
ETTm1	96	0.305	0.353	<u>0.278</u>	<u>0.328</u>	0.264	0.318	0.327	0.365	0.327	0.361	0.326	0.364	0.309	0.352	0.326	0.361	0.334	0.368	0.329	0.367	0.338	0.375
	192	0.328	0.370	<u>0.320</u>	<u>0.359</u>	0.311	0.352	0.363	0.387	0.366	0.383	0.367	0.383	0.355	0.378	0.363	0.384	0.377	0.391	0.367	0.385	0.374	0.387
	336	0.349	0.384	<u>0.338</u>	<u>0.371</u>	0.332	0.368	0.389	0.407	0.398	0.404	0.402	0.409	0.387	0.399	0.395	0.406	0.426	0.420	0.399	0.410	0.410	0.411
	720	0.392	0.416	<u>0.383</u>	<u>0.404</u>	0.372	0.399	0.457	0.445	0.464	0.437	0.469	0.446	0.448	0.435	0.456	0.441	0.491	0.459	0.454	0.439	0.478	0.450
	Avg	0.344	0.381	<u>0.330</u>	<u>0.366</u>	0.320	0.359	0.384	0.401	0.389	0.396	0.391	0.401	0.375	0.391	0.385	0.398	0.407	0.410	0.387	0.400	0.400	0.406
ETTm2	96	0.165	0.255	<u>0.155</u>	<u>0.250</u>	0.150	0.243	0.178	0.262	0.176	0.259	0.178	0.260	0.171	0.255	0.177	0.258	0.180	0.264	0.175	0.259	0.187	0.267
	192	0.217	0.297	<u>0.215</u>	<u>0.294</u>	0.214	0.292	0.244	0.308	0.242	0.302	0.242	0.303	0.238	0.300	0.243	0.301	0.250	0.309	0.241	0.302	0.249	0.309
	336	0.262	0.330	<u>0.258</u>	<u>0.318</u>	0.253	0.312	0.305	0.346	0.298	0.337	0.303	0.342	0.301	0.340	0.302	0.340	0.311	0.348	0.305	0.343	0.321	0.351
	720	0.333	0.379	<u>0.329</u>	<u>0.368</u>	0.328	0.364	0.402	0.404	0.396	0.394	0.400	0.399	0.401	0.397	0.404	0.398	0.412	0.407	0.402	0.400	0.408	0.403
	Avg	0.244	0.315	<u>0.239</u>	<u>0.308</u>	0.236	0.303	0.282	0.330	0.278	0.323	0.281	0.326	0.278	0.323	0.281	0.324	0.288	0.332	0.281	0.326	0.291	0.333
ETT1	96	0.362	0.395	<u>0.357</u>	<u>0.386</u>	0.342	0.375	0.374	0.391	0.375	0.392	0.375	0.398	0.377	0.397	0.378	0.395	0.386	0.405	0.414	0.419	0.384	0.402
	192	0.406	0.427	<u>0.392</u>	<u>0.413</u>	0.384	0.404	0.421	0.421	0.430	0.422	0.427	0.429	0.425	0.425	0.435	0.424	0.441	0.436	0.460	0.445	0.436	0.429
	336	0.436	0.449	<u>0.420</u>	<u>0.435</u>	0.407	0.428	0.464	0.440	0.471	0.443	0.472	0.450	0.457	0.441	0.485	0.447	0.487	0.458	0.501	0.466	0.491	0.469
	720	0.471	0.482	<u>0.436</u>	<u>0.450</u>	0.418	0.436	0.466	0.462	0.478	0.464	0.476	0.474	0.464	0.463	0.496	0.472	0.503	0.491	0.500	0.488	0.521	0.500
	Avg	0.419	0.438	<u>0.401</u>	<u>0.421</u>	0.388	0.411	0.431	0.429	0.438	0.430	0.438	0.438	0.431	0.432	0.448	0.435	0.454	0.448	0.469	0.455	0.458	0.450
ETT2	96	0.278	0.339	<u>0.271</u>	<u>0.327</u>	0.264	0.320	0.293	0.343	0.287	0.338	0.293	0.345	0.289	0.340	0.291	0.342	0.297	0.349	0.302	0.348	0.340	0.374
	192	0.336	0.381	<u>0.335</u>	<u>0.376</u>	0.332	0.364	0.375	0.396	0.367	0.388	0.367	0.394	0.370	0.391	0.372	0.390	0.380	0.400	0.388	0.400	0.402	0.414
	336	0.373	0.410	<u>0.364</u>	<u>0.402</u>	0.360	0.399	0.429	0.441	0.410	0.424	0.419	0.431	0.422	0.434	0.419	0.431	0.428	0.432	0.426	0.433	0.452	0.452
	720	0.411	0.441	<u>0.391</u>	<u>0.428</u>	0.382	0.423	0.466	0.468	0.421	0.440	0.427	0.445	0.429	0.445	0.431	0.450	0.427	0.445	0.431	0.446	0.462	0.468
	Avg	0.350	0.393	<u>0.340</u>	<u>0.383</u>	0.335	0.377	0.391	0.412	0.371	0.397	0.377	0.404	0.378	0.403	0.378	0.403	0.383	0.407	0.387	0.407	0.414	0.427
Weather	96	0.148	0.204	<u>0.144</u>	<u>0.197</u>	0.141	0.184	0.164	0.210	0.174	0.221	0.166	0.207	0.168	0.209	0.163	0.207	0.174	0.214	0.177	0.218	0.172	0.220
	192	0.189	0.243	<u>0.184</u>	<u>0.241</u>	0.182	0.240	0.209	0.250	0.219	0.259	0.216	0.254	0.220	0.254	0.224	0.258	0.221	0.254	0.255	0.259	0.219	0.261
	336	0.233	0.278	<u>0.230</u>	<u>0.276</u>	0.224	0.272	0.264	0.290	0.273	0.296	0.273	0.296	0.276	0.296	0.278	0.298	0.278	0.296	0.278	0.297	0.280	0.306
	720	0.289	0.320	<u>0.287</u>	<u>0.318</u>	0.280	0.306	0.343	0.342	0.349	0.345	0.351	0.346	0.353	0.347	0.357	0.350	0.358	0.349	0.354	0.348	0.365	0.359
	Avg	0.215	0.261	<u>0.211</u>	<u>0.258</u>	0.207	0.251	0.245	0.273	0.254	0.280	0.252	0.276	0.254	0.277	0.256	0.278	0.258	0.278	0.266	0.281	0.259	0.287
Electricity	96	0.206	0.294	0.142	0.235	0.124	0.218	0.174	0.266	0.147	0.251	<u>0.139</u>	<u>0.234</u>	0.151	0.247	0.148	0.242	0.148	0.240	0.195	0.285	0.168	0.272
	192	0.247	0.338	0.168	0.255	0.149	0.236	0.182	0.273	0.176	0.262	<u>0.156</u>	<u>0.249</u>	0.165	0.261	0.165	0.257	0.162	0.253	0.199	0.289	0.184	0.289
	336	0.310	0.398	0.188	0.271	0.164	0.252	0.197	0.286	0.193	0.281	<u>0.172</u>	<u>0.267</u>	0.183	0.280	0.180	0.274	0.178	0.269	0.215	0.305	0.198	0.300
	720	0.383	0.455	0.192	0.277	<u>0.205</u>	<u>0.288</u>	0.236	0.320	0.232	0.329	0.209	0.299	0.220	0.309	0.218	0.305	0.225	0.317	0.256	0.337	0.220	0.320
	Avg	0.287	0.371	0.173	<u>0.260</u>	0.161	0.249	0.197	0.286	0.187	0.281	<u>0.169</u>	0.262	0.180	0.274	0.178	0.270	0.178	0.270	0.216	0.304	0.193	0.295
Traffic	96	0.591	0.401	<u>0.375</u>	<u>0.262</u>	0.358	0.246	0.423	0.286	0.443	0.298	0.426	0.292	0.416	0.280	0.403	0.274	0.395	0.268	0.544	0.359	0.593	0.321
	192	0.623	0.431	<u>0.388</u>	<u>0.265</u>	0.379	0.248	0.442	0.295	0.496	0.323	0.439	0.298	0.435	0.288	0.429	0.289	0.417	0.276	0.540	0.354	0.617	0.336
	336	0.697	0.485	<u>0.397</u>	0.285	0.386	0.262	0.473	0.335	0.520	0.330	0.449	0.307	0.451	0.296	0.441	0.295	0.433	<u>0.283</u>	0.551	0.358	0.629	0.336
	720	0.782	0.528	<u>0.451</u>	0.332	0.427	0.282	0.481	0.357	0.540	0.344	0.475	0.309	0.484	0.314	0.463	<u>0.300</u>	0.467	0.302	0.586	0.375	0.640	0.350
	Avg	0.673	0.461	<u>0.403</u>	0.286	0.388	0.260	0.455	0.318	0.500	0.324	0.447	0.302	0.447	0.295	0.434	0.289	0.428	<u>0.282</u>	0.555	0.362	0.620	0.336
1 st Count	0	0	<u>1</u>	<u>1</u>	34	34	0	0	0	0	0	0	0	0	0	0	0	0	0	0	0	0	0

FLAME: Flow Enhanced Legendre Memory Models for General Time Series Forecasting

Table 16. Probabilistic forecasting results. Full-shot, 10% few-shot and zero-shot results of FLAME Small v.s most advanced end-to-end supervised models on commonly-used datasets in ProbTS. Lower CRPS or NMAE values indicate better predictions. **Red**: the best, **Blue**: the second best.

Models	FLAME Small (Zero-shot)		FLAME Small (10% few-shot)		FLAME Small (Full-shot)		NSDIFF (2025)		K ² VAE (2025)		TSDiff (2023)		CSDI (2022)		TimeGrad (2022)		GRU NVP (2021)		
	CRPS	NMAE	CRPS	NMAE	CRPS	NMAE	CRPS	NMAE	CRPS	NMAE	CRPS	NMAE	CRPS	NMAE	CRPS	NMAE	CRPS	NMAE	
ETTm1	96	0.294	0.368	<u>0.233</u>	<u>0.287</u>	0.211	0.275	0.295	0.364	0.235	0.294	0.344	0.441	0.236	0.308	0.522	0.645	0.383	0.488
	192	0.332	0.420	<u>0.259</u>	<u>0.317</u>	0.232	0.298	0.285	0.350	0.261	0.330	0.345	0.441	0.291	0.377	0.603	0.748	0.396	0.514
	336	0.341	0.427	0.292	0.351	0.279	<u>0.355</u>	<u>0.289</u>	0.357	0.304	0.386	0.462	0.571	0.322	0.419	0.601	0.759	0.486	0.630
	720	0.364	0.454	0.304	0.392	0.282	0.358	0.411	0.500	<u>0.302</u>	<u>0.387</u>	0.478	0.622	0.448	0.578	0.621	0.793	0.546	0.707
	Avg	0.333	0.417	<u>0.272</u>	<u>0.337</u>	0.251	0.322	0.320	0.393	0.276	0.349	0.407	0.519	0.324	0.421	0.587	0.736	0.453	0.585
ETTm2	96	0.120	0.153	0.117	<u>0.144</u>	0.114	0.141	0.145	0.176	0.128	0.148	0.175	0.224	<u>0.115</u>	0.146	0.427	0.525	0.319	0.413
	192	0.146	0.182	<u>0.145</u>	0.178	0.138	<u>0.166</u>	0.162	0.196	0.161	0.163	0.255	0.316	0.147	0.189	0.424	0.530	0.326	0.427
	336	0.163	0.202	<u>0.160</u>	0.199	0.151	0.182	0.172	0.209	0.180	<u>0.183</u>	0.328	0.397	0.190	0.248	0.469	0.566	0.449	0.580
	720	0.185	<u>0.223</u>	<u>0.181</u>	0.231	0.170	0.211	0.364	0.428	0.224	0.224	0.344	0.416	0.239	0.306	0.470	0.561	0.561	0.749
	Avg	0.154	0.190	<u>0.151</u>	0.188	0.143	0.175	0.211	0.252	0.173	<u>0.180</u>	0.276	0.338	0.173	0.222	0.448	0.546	0.414	0.542
ETTth1	96	0.265	0.322	<u>0.254</u>	<u>0.311</u>	0.247	0.301	0.301	0.380	0.280	0.358	0.395	0.510	0.437	0.557	0.455	0.585	0.379	0.481
	192	0.288	0.346	<u>0.272</u>	<u>0.336</u>	0.268	0.322	0.309	0.386	0.304	0.392	0.467	0.596	0.496	0.625	0.516	0.680	0.425	0.531
	336	0.300	0.371	<u>0.297</u>	<u>0.369</u>	0.288	0.363	0.357	0.448	0.326	0.413	0.450	0.581	0.454	0.574	0.512	0.666	0.458	0.580
	720	0.320	0.402	<u>0.308</u>	<u>0.395</u>	0.300	0.392	0.384	0.513	0.331	0.428	0.516	0.657	0.528	0.657	0.523	0.672	0.502	0.643
	Avg	0.293	0.360	<u>0.283</u>	<u>0.353</u>	0.276	0.345	0.337	0.432	0.310	0.398	0.457	0.586	0.479	0.603	0.502	0.651	0.441	0.559
ETTth2	96	0.139	0.177	<u>0.133</u>	<u>0.175</u>	0.122	0.162	0.175	0.220	0.182	0.206	0.336	0.421	0.164	0.214	0.358	0.448	0.432	0.548
	192	0.152	0.195	<u>0.148</u>	<u>0.193</u>	0.137	0.188	0.200	0.245	0.185	0.220	0.265	0.339	0.226	0.294	0.457	0.575	0.625	0.766
	336	0.170	0.216	<u>0.167</u>	<u>0.209</u>	0.155	0.194	0.207	0.257	0.245	0.277	0.350	0.427	0.274	0.353	0.481	0.606	0.793	0.942
	720	0.183	0.231	<u>0.177</u>	<u>0.228</u>	0.171	0.222	0.209	0.260	0.237	0.272	0.406	0.482	0.302	0.382	0.445	0.550	0.539	0.688
	Avg	0.161	0.205	<u>0.156</u>	<u>0.201</u>	0.146	0.192	0.198	0.246	0.212	0.244	0.339	0.417	0.242	0.311	0.435	0.545	0.597	0.736
Weather	96	0.071	0.088	0.069	<u>0.085</u>	0.065	0.083	0.123	0.129	0.083	0.087	0.104	0.113	<u>0.068</u>	0.087	0.130	0.164	0.116	0.145
	192	0.089	0.113	0.078	0.101	<u>0.073</u>	<u>0.088</u>	0.132	0.132	0.085	0.090	0.134	0.144	0.068	0.086	0.127	0.158	0.122	0.147
	336	0.094	0.121	<u>0.082</u>	0.114	0.075	0.089	0.130	0.128	0.087	<u>0.091</u>	0.137	0.138	0.083	0.098	0.130	0.162	0.128	0.160
	720	0.103	0.132	<u>0.098</u>	0.119	0.091	<u>0.096</u>	0.142	0.147	<u>0.090</u>	0.094	0.152	0.141	0.087	0.102	0.113	0.136	0.110	0.135
	Avg	0.089	0.114	0.082	0.105	0.076	0.089	0.132	0.134	0.086	<u>0.091</u>	0.132	0.134	<u>0.077</u>	0.093	0.125	0.155	0.119	0.147
Electricity	96	0.071	0.090	<u>0.069</u>	<u>0.088</u>	0.069	0.088	0.160	0.202	0.089	0.093	0.344	0.441	0.153	0.203	0.096	0.119	0.094	0.118
	192	0.086	0.103	0.083	<u>0.097</u>	<u>0.084</u>	0.095	0.248	0.358	0.097	0.102	0.345	0.441	0.200	0.264	0.100	0.124	0.097	0.121
	336	<u>0.096</u>	0.125	0.097	0.116	0.094	<u>0.114</u>	0.252	0.362	0.101	0.105	0.462	0.571	/	/	0.102	0.126	0.099	0.123
	720	0.117	0.154	0.108	0.123	0.104	<u>0.117</u>	0.259	0.368	<u>0.105</u>	0.110	0.478	0.622	/	/	0.108	0.134	0.114	0.144
	Avg	0.093	0.118	<u>0.089</u>	0.106	0.088	<u>0.104</u>	0.230	0.322	0.098	0.103	0.407	0.519	/	/	0.102	0.126	0.101	0.127
Traffic	96	0.240	0.293	0.227	0.262	0.203	0.217	0.393	0.500	0.216	<u>0.222</u>	0.294	0.342	/	/	<u>0.202</u>	0.234	0.187	0.231
	192	0.257	0.319	0.243	0.289	0.212	0.223	0.448	0.585	0.220	<u>0.227</u>	0.306	0.354	/	/	<u>0.208</u>	0.239	0.192	0.236
	336	0.271	0.341	0.266	0.317	0.220	0.228	0.455	0.592	0.228	<u>0.235</u>	0.317	0.392	/	/	<u>0.213</u>	0.246	0.201	0.248
	720	0.304	0.395	0.288	0.322	0.231	0.237	0.452	0.588	0.235	<u>0.242</u>	0.391	0.478	/	/	<u>0.220</u>	0.263	0.211	0.264
	Avg	0.268	0.337	0.256	0.298	0.217	0.226	0.437	0.566	0.225	<u>0.232</u>	0.327	0.392	/	/	<u>0.211</u>	0.246	0.198	0.245
Exchange	96	<u>0.023</u>	<u>0.028</u>	0.024	0.031	0.022	0.027	0.023	0.029	0.027	0.028	0.079	0.090	0.028	0.036	0.068	0.079	0.071	0.091
	192	0.032	0.037	<u>0.028</u>	<u>0.036</u>	0.025	0.031	0.029	0.037	0.035	0.036	0.093	0.106	0.045	0.058	0.087	0.100	0.068	0.087
	336	0.044	0.049	0.035	0.037	<u>0.031</u>	<u>0.033</u>	0.043	0.053	0.027	0.028	0.081	0.106	0.060	0.076	0.074	0.086	0.072	0.091
	720	0.074	0.079	0.067	0.074	0.053	0.070	<u>0.057</u>	<u>0.071</u>	0.081	0.083	0.082	0.142	0.143	0.173	0.099	0.113	0.079	0.103
	Avg	0.043	0.048	0.039	0.045	0.033	0.040	<u>0.038</u>	0.047	0.043	<u>0.044</u>	0.084	0.111	0.069	0.086	0.082	0.095	0.073	0.093
ILI	24	0.135	0.166	0.112	0.133	0.088	0.103	<u>0.092</u>	<u>0.108</u>	0.110	0.113	0.228	0.242	0.250	0.263	0.275	0.296	0.257	0.283
	36	0.164	0.200	0.148	0.185	0.137	<u>0.168</u>	0.151	0.178	<u>0.140</u>	0.144	0.235	0.246	0.285	0.298	0.272	0.298	0.281	0.307
	48	0.176	0.216	0.169	0.205	0.142	<u>0.171</u>	<u>0.151</u>	0.178	0.153	0.157	0.265	0.275	0.285	0.301	0.295	0.320	0.288	0.314
	60	0.171	0.211	0.165	0.198	0.152	<u>0.184</u>	0.168	0.198	<u>0.164</u>	0.167	0.263	0.272	0.283	0.299	0.295	0.325	0.307	0.333
	Avg	0.162	0.198	0.149	0.180	0.130	<u>0.157</u>	<u>0.140</u>	0.165	0.142	0.145	0.248	0.259	0.276	0.290	0.284	0.310	0.283	0.309
1 st Count	0	0	1	1	28	26	0	0	1	8	0	0	2	1	0	0	4	0	

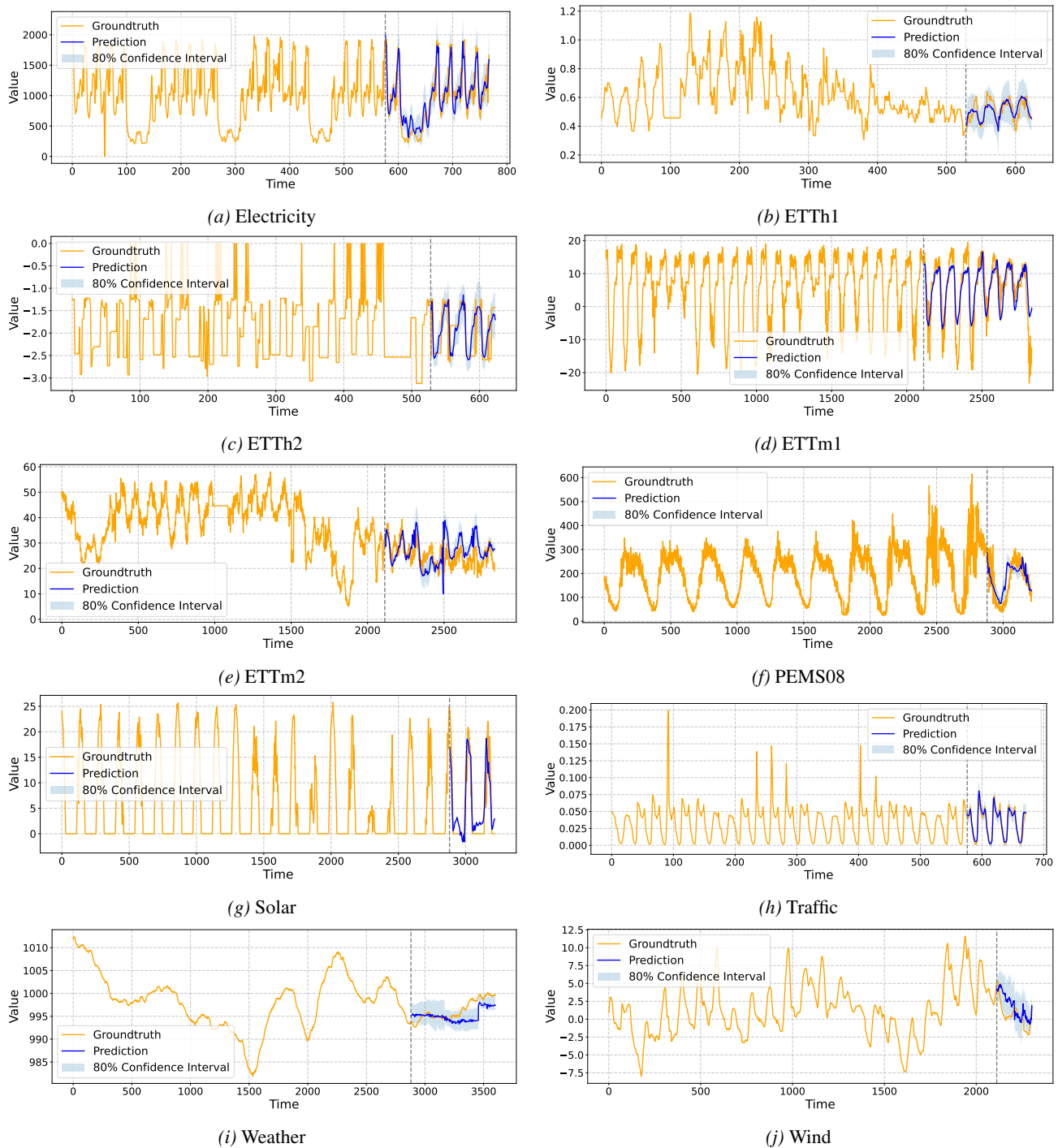


Figure 8. Visualization of TFSM-Bench

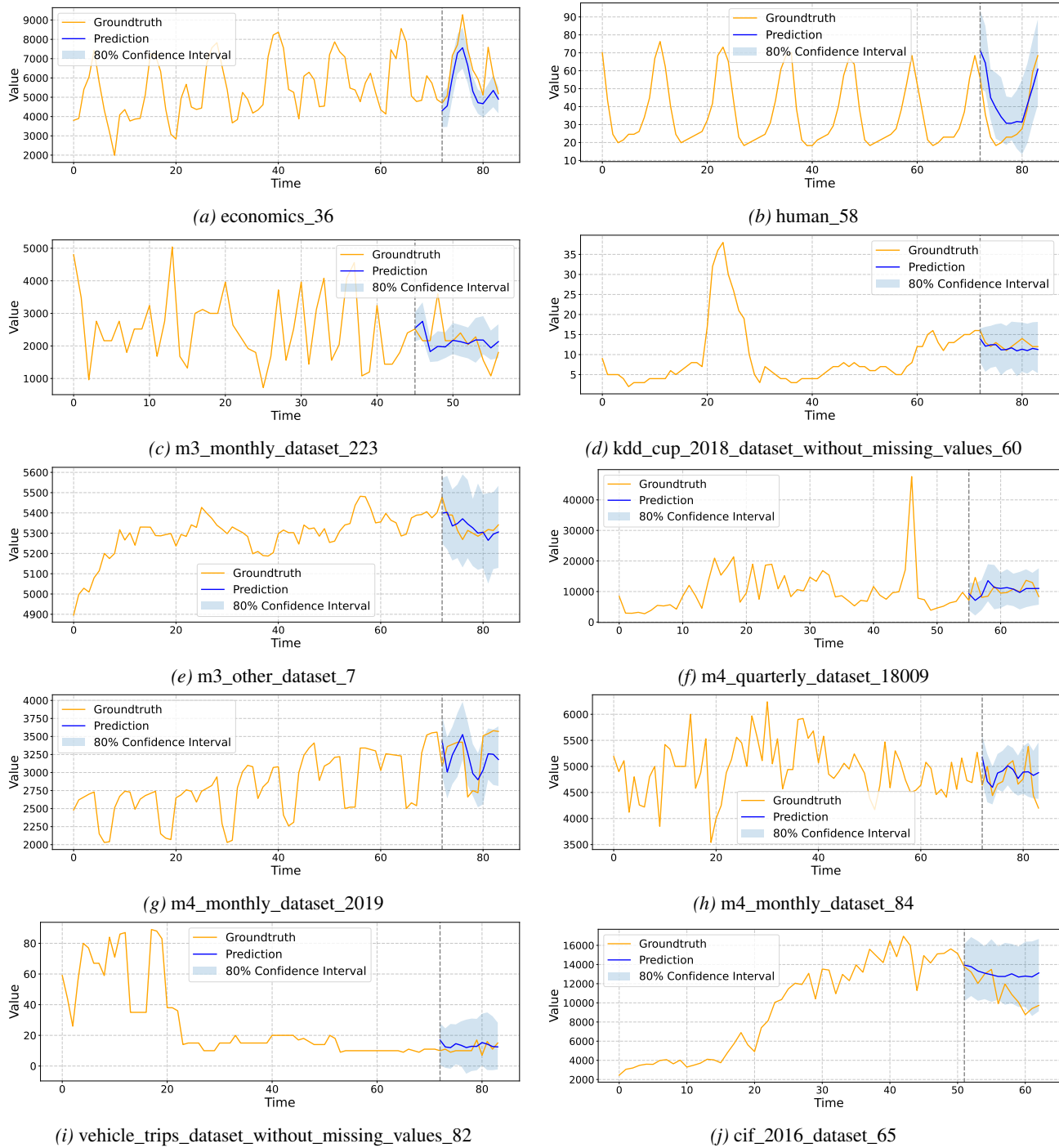


Figure 9. Visualization of Univariate Datasets in TFB

E. Related Works

Time Series Analysis holds a position of paramount importance across a diverse range of fields, including the economy (Qiu et al., 2025b;a; Liu et al., 2025a), transportation (Wu et al., 2025d; 2024), health (Lu et al., 2023; 2024a;b), weather (Li et al., 2025a; Yang et al., 2024; Zhou et al., 2025), and energy (Sun et al., 2025a). It encompasses a multitude of critical tasks, such as forecasting (Li et al., 2025b; Dai et al., 2024c), anomaly detection (Wang et al., 2025a; Qiu et al., 2025c; Wu et al., 2025c; Zhang et al., 2025), classification (Liu et al., 2024b), imputation (Wu et al., 2023), and others (Qiu et al., 2025f; Wu et al., 2025b). Among these tasks, Time Series Forecasting is the one most extensively applied in practical, real-world scenarios.

Time series forecasting (TSF) involves the prediction of future observations on the basis of historical data. Research results have demonstrated that features learned through specific methods may present superior performance in comparison to human-designed features (Dai et al., 2024b; Hu et al., 2025a; Dai et al., 2024c; Liu et al., 2025c; Sun et al., 2025b;a; Niu et al., 2025; Qiu et al., 2025d). By leveraging the representation learning capabilities of deep neural networks (DNNs), numerous deep-learning based approaches have come into existence. For example, TimesNet (Wu et al., 2023) and SegRNN (Lin et al., 2023) model time series as vector sequences, utilizing CNNs or RNNs to capture temporal dependencies. Furthermore, Transformer architectures, including Informer (Zhou et al., 2021), Dsformer (Yu et al., 2023), TimeFilter (Hu et al., 2025b), TimeBridge (Liu et al., 2025b), PDF (Dai et al., 2024a), Triformer (Cirstea et al., 2022), PatchTST (Nie et al., 2023), ROSE (Wang et al., 2025c), LightGTS (Wang et al., 2025b), and MagicScaler (Pan et al., 2023), are able to more precisely capture the complex relationships between time points, thus significantly improving forecasting performance. MLP-based methods, such as DUET (Qiu et al., 2025e), SRSNet (Wu et al., 2025a), APN (Liu et al., 2026), AMD (Hu et al., 2025a), NLinear (Zeng et al., 2023), and DLinear (Zeng et al., 2023), adopt relatively simpler architectures with fewer parameters yet still succeed in achieving highly competitive forecasting accuracy.